SPHERICAL REFLECTOR FEED FIELD SYNTHESIS

BY GEOMETRICAL OPTICS

AND SPHERICAL WAVE EXPANSION

by

EDWARD F. MCCANN, II

S.B., UNITED STATES NAVAL ACADEMY

(1965)

SUBMITTED TO THE DEPARTMENT OF NAVAL ARCHITECTURE AND MARINE

ENGINEERING IN PARTIAL FULFILLMENT OF THE REQUIREMENTS OF

THE MASTER OF SCIENCE DEGREE IN ELECTRICAL ENGINEERING

AND THE PROFESSIONAL DEGREE, NAVAL ENGINEER

at the

MASSACHUSETTS INSTITUTE OF TECHNOLOGY

May, 1970

Signature of Author .... Signature redacted ....

Department of Naval Architecture and
Marine Engineering, May, 1970

Certified by .... Signature redacted ....
Thesis Supervisor

Certified by .... Signature redacted ....
Reader for the Department

Accepted by .... Signature redacted ....
Chairman, Departmental Committee on Graduate Students

ABSTRACT

The inherent symmetry of a spherical reflector microwave antenna
suggests that if the fields incident upon the reflector from a feed
required to produce a specified reflected field can be determined,
then scanning of this reflected field may be accomplished by rotation
of the feed assembly rather than by rotation of the entire antenna.
A technique has been determined to solve for the fields in vicinity
of a hypothetical transmitting feed that will, following reflection
from the surface of the spherical reflector, yield a specified field
pattern at the reflector aperture. From given fields over a sphere,
a portion of which coincides with the surface of the spherical reflec-
tor, a spherical harmonic series expansion is used to calculate the
fields on a smaller concentric sphere encompassing the feed region
in solution of the boundary value problem.

This technique is extended to a case where it is shown that
geometrical optics approximations are valid over a specific region
of the reflector system, and that by ray tracing, the fields on an
arbitrary reference sphere, whose radius is confined only to the
axis of symmetry of the reflector, can be determined. From this
field distribution, the spherical harmonic series expansion can be
used to determine the fields on the surface of a smaller concentric
sphere enclosing the hypothetical feed. It is shown that this tech-
nique has flexibility wherein a number of origins could be examined
for various feed spheres with fewer terms of the series expansion
than with the fixed-origin case.

TABLE OF CONTENTS

ACKNOWLEDGEMENT

Expressions of gratitude and appreciation are due Professor L. J. Chu for suggestion of this thesis topic and for subsequent guidance throughout the study. The **same** thanks and appreciation are due Dr. L. J. Ricardi of Lincoln Laboratories for a number of hours spent in consultation, guidance and computation.

CHAPTER I

GENERAL BACKGROUND

1.1   The fact that a reflecting paraboloid of revolution, when il-
luminated by a source of spherical waves placed at the geometrical
focus of the paraboloid, will produce a uniform plane wave over the
aperture of the reflector is well known. The generation of a pencil-
shaped beam antenna pattern has reached a state of refinement such
that extremely narrow beamwidth, low sidelobe levels, reasonably
broad-band operation, high aperture efficiency and gain are readily
attainable for many applications.

The axis of this pencil beam coincides with the axis of revolution
of the reflector, and attempts to direct the antenna pattern by off-
axis movement of the point-source feed have failed for all but the
smallest off-axis angles. Therefore, to direct the pattern requires
that the entire reflector and feed assembly be rotated or moved to aim
the antenna pattern in the direction of interest.

Widespread use of large aperture paraboloidal reflectors with wide-
angle scanning requirements has stimulated considerable interest in
development of improved feed systems to alleviate problems of ground
noise radiation, spurious polarization effects and low aperture ef-
ficiencies encountered in radio-telescope applications. Other such
problems that are encountered include difficulties in maintaining
mechanical and structural tolerances of the reflecor surface at partic-
ular frequencies of interest.

The inherent symmetry of the spherical reflector suggests that it could provide some relief from the problems previously described. Assuming an energy source could be obtained that would, upon reflection from the spherical surface, provide an antenna pattern whose beam coincided with the radius of the reflector upon which illumination occurred, it would be no longer necessary to overcome the inertia of the entire system to meet a wide-angle scanning requirement, but merely to direct the feed assembly as desired. In such a case, it is feasible that large apertures could be illuminated to provide desired gain . Further, the symmetry of a spherical section enhances both ease of fabrication and verification of system tolerances in many applications. Other advantages that may be realized from such a system follow directly from speculation of possible application, including for example an antenna system whose reflector could be imbedded in the earth, with few moving parts, presenting a low silhouette to wind forces.

Unfortunatly, analysis of the spherical reflector reveals its inherent spherical aberration. For a plane wave incident upon a spherical reflector, rays close to the axis of symmetry intersect at a point defined as the paraxial focus, exactly half-way between the center of curvature of the spherical section and the vertex. Other rays reflected from the surface intersect the axis at points closer to the vertex. This phenomenon may be observed in figure 1, where rays are constrained by Snell's law to reflect with an angle equal to that of incidence, as measured from the surface normal at the point of interest. A more complete explanation of this reflection phenomenon will be given

figure 1.
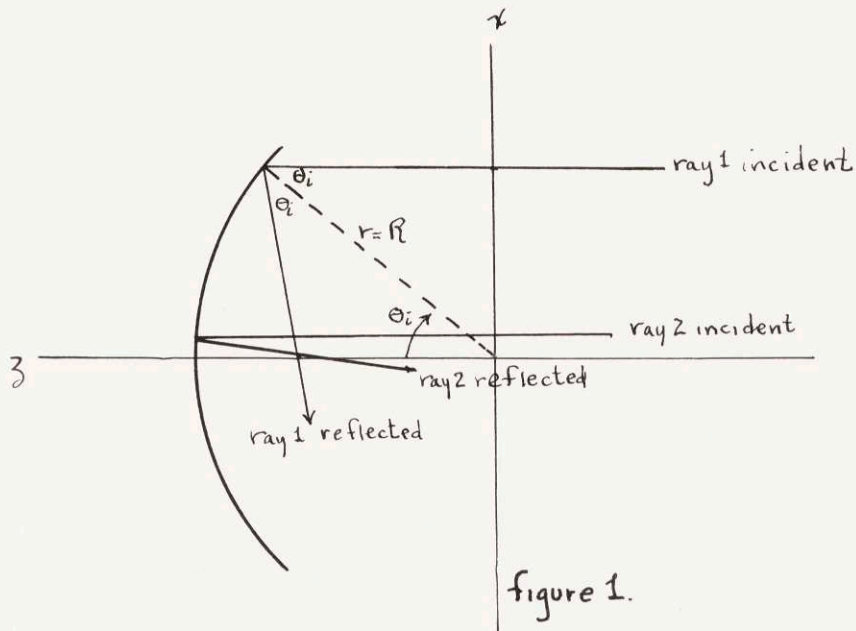
This suggests that rather than a distinct point focus there exists a
fuzzy focal region. Illumination of the reflector with a point source in
the focal region reveals a diffraction pattern with wider beamwidth,
higher sidelobes and much less gain than a paraboloidal reflector of
identical aperture. It is this aberration that has presented an obstacle
to development of the spherical rather than paraboloidal reflector for
use as a microwave antenna. Since introduction of the problem to the
microwave community in World War II, however, there has remained an
active interest in the problem. Most recently, with construction in
1960 of the Arecibo (Puerto Rico) Ionospheric Observatory's 1000-feet
diameter spherical reflector[1], considerable interest has been generated
in the solution to problems of spherical aberration at radio frequencies
by means of various feed systems.

1.2 It is appropriate to review past efforts relevant to the problem. Early
attempts to explain optical phenomena followed from geometrical theory.
Euclid presented an analysis of the reflection laws around 300 B.C. while
observing that light energy could be concentrated by means of

8

reflectors.[2] Early astronomers used spherical mirrors as primary collectors of light incident upon their telescopes. Presumably the ease of manufacture of these spherical mirrors led to their widespread use, even though the geometrical analysis of the reflecting properties of paraboloidal surfaces had been conducted. The difficulty of manufacture of the latter apparently precluded exploiting their point-focus characteristic.

The concept of a spherical reflector for microwave use evolved from the World War II advances of radar technology. In 1941, Ashmead and Pippard suggested two approaches to the aberration encountered:

1. For reflectors of large radius and restricted aperture, the surface of the spherical reflector departs only slightly from that of a paraboloidal reflector. It follows that the diffraction pattern is only slightly different from that of a paraboloidal reflector. If the slight departure from plane wave illumination at the aperture and the value of gain accompanying the restrictive aperture can be tolerated, this approach permits a simple design and is suitable for wide angles of scan.

2. For the general case of spherical reflectors,
   should the primary energy source be a special
   radiator that provides not spherical waves but
   waves whose departure from spherical waves is
   just that necessary to compensate for the differ-
   ence between the sphere and paraboloid, then
   reflected wave fronts will be plane waves, uniform-
   ly illuminating the aperture.

Early work indicated that it was possible to create non-spherical
waves of approximately the right shape by proper combination of wave-
guide horns and dielectric lenses. Unfortunatly, difficulties in
correcting for the larger phase error did not, at the time, justify
pursuance of this approach. Rather, to meet the expedience of the
wartime effort, the first approach of toleration of error rather than
compensation was used exclusively. Subsequent studies exploiting this
technique reached a natural conclusion with the work of Li[4], who
extended and verified the theory of restrictive aperture large radius
spherical reflectors. His experimental work indicated that with a ten-
foot aperture hemisphere absolute gain comparable to that of a forty-
inch paraboloid was obtained over a scan of 140° with rotation of
the feed at a constant radius from the reflector.

The second, more interesting approach to the solution allows the
use of a larger aperture at the expense of increased complexity in
cost, design and some reduction in the available angle of scan.

In the context of the latter approach corrective devices have fallen into the following categories:

1. lens structures
2. auxilary reflectors
3. line-source feeds
4. transverse aperture feeds

Lens structures, while providing satisfactory correction at optical frequencies, provide marginal correction in microwave applications. Sizes comparable to the reflector and primary source, requirements for large pieces of carefully controlled precision-cut dielectric and inherent dielectric losses, to say nothing of the costs and weights involved, relegate this category of corrective devices at microwave frequencies to a position of academic interest.

Auxilary reflectors are of minor interest when the undesirable characteristics of shadowing or aperture blockage are imminent. Even in cases where this is of small concern, the excessive weight of the secondary reflector must be considered, as must the mechanical arrangements for support of the assembly. A gregorian reflector has been described by Holt and Bouche[5] wherein a reflecting surface intercepting a great deal of the energy incident from the spherical reflector is installed. The surface of the sub-reflector is such that it provides a constant path length from some reference plane near the aperture to the primary source.

Experimental results indicate that the scanning capability was realized to 30° by rotation of the sub-reflector on a constant radius from the spherical surface. Sidelobe levels were very high in comparison to those available with paraboloidal reflectors. While aperture blockage was estimated to be 1.5%, no figures on gain were given.

The earliest attempts at compensation involved the fact that rays incident upon the spherical reflector were reflected to cross the axis of symmetry. It was postulated by Spencer, Sletten and Walsh[6] that the incoming energy could be recombined with an appropriate phase shift to provide a maximum of received signal. Reciprocity was invoked to suggest that a properly phased line source could produce a wavefront that would provide uniform illumination over the aperture. Techniques of geometrical optics were used for path length calculations. The sources considered were open-ended waveguides, polyrod travelling wave structures, discrete dipole sources alog the axis and slotted waveguide feeds. Indeed, the first feed system constructed at the Arecibo reflector was based upon a modification of this design[7]. Aberrationless scan of over 60° was predicted for this initial installation-as well as reasonable aperture efficiency. Actual results were well under those anticipated. The high-power dual circularly polarized feed illuminated the full aperture of 1000 feet with an efficiency of 21% at 430 MHz[8]. Love[9] described a composite radiating system wherein channel guide feed and a polyrod array provided a travelling wave structure to illuminate from both the line focus and the paraxial focus. He predicted a scan of 110° for a hemispherical reflector, and efficiency on the order of

12

55%. Schell[10] investigated the fields along the axis by application of diffraction theory. He demonstrated the deviation from the geometrical optics solution in the non-zero wavelength and agreement in the zero-wavelength case. Schell's solution consisted of the use of a sufficient number of discrete sources located along the axis, illuminating particular regions of the reflector. The analysis was based upon the fields present along the focal axis when the reflector was illuminated by an incoming plane wave. In an attempt to solve the problem based upon Schell's solution, Cohen and Perona[11] constructed a feed system at the Arecibo reflector. Their compound antenna feed consisted of a four-element linear array with a reflecting screen and a sixteen-element linear array located on the axis. Experimentation determined that gain was lower and sidelobes higher than had been anticipated. Aperture efficiencies were on the order of 30-38%[12]. McCormick[13] followed this study with an analysis that considered the transmitting case and, in particular, the aspect of polarization. His analysis concluded that a gain deterioration was inevitable with a circular waveguide with circumferential slots that did not consider the azimuthal fields as well as the longitudinal fields. The theory of McCormick was used by Love and Gustinic[14] to illustrate the feasibility of illuminating from a leaky cylindrical waveguide that considered these fields. Most recent literature indicates that a line source feed with high performance has finally been achieved at Arecibo. LaLonde and Harris[15] note that their feed has been installed at the observatory and has realized an

overall efficiency of 70% at 318 MHz. Designing for a flat waveguide line feed with transverse slots was necessary to avoid problems of previous feeds which, it was felt, did not provide sufficient control over amplitude and phase variation along the line focus nor sufficient isolation from the effects of mutual coupling between the radiating elements of the feed. The lower frequency of operation was specified to avoid losses due to surface imperfections of the reflector. The design of the phase and amplitude required was based upon a geometrical optics analysis of the rays intersecting the axis. This design is significant in that it represents the first installation of a corrective feed in a spherical reflector that has yielded aperture efficiencies approaching those of paraboloidal reflectors. Aside from strengthening arguments for fixed-reflector scanning antennas, providing some 40° of scan with high efficiency at Arecibo, the success of this feed indicates the potential of the spherical reflector antenna for fully steerable arrays, where desired.

It has been noted by Ricardi[16] that line source radiator correcting feed systems must be capable of producing a wave whose polarization and shape are not easily obtained with elementary radiators. This basic fact has caused present day line source correcting feeds to fall short of expectations, with exception of the LaLonde-Harris feed. It should be noted, however, that the requirements of Arecibo call for high power with capability for dual circular polarization[17]. The line feed of LaLonde and Harris achieved success in providing for linear polarization. While the high power requirement may be easily met with the slotted guide,

the authors note that polarization flexibility has yet to be developed. Presumably, the transverse aperture corrective feed designs have no inherent difficulty in polarization flexibility. Early attempts to provide aperture corrective feeds met with reasonable success in over-coming the aberration, but were hampered by aperture blockage of the moderately large feed systems. Sletten and Mavroides[18] were succesful in lowering sidelobes substantially, while plagued with aperture blockage. An aperture feed was suggested for the spherical reflector by Burrows and Ricardi[19] in which they predicted a possible gain of 61 db. compared to the maximum gain of such an aperture the size of Arecibo at 62.8 db. Their feed system was derived from a spherical harmonic expan-sion of the fields necessary to produce a uniform distribution over the aperture, based upon the fields incident upon a spherical reflector. Spencer and Hyde[20] conducted a detailed study of the focal region fields associated with the spherical reflector illuminated by incoming plane waves and concluded that only a vector field solution considering polar-ization would yield adequate information. They solved the diffraction integral by means of a stationary phase approximation, noting the similarities to the geometrical optics approximations. Their theory was shown to have reasonable agreement with fields actually found in the focal region by experimentation, and their work has been used as a basis for further study into aperture feeds[21]. Their work, however, did not offer a solution to the problem, but rather provided a theoretical analysis of the fields that could be expected. Work by Minnet and MacA. Thomas[22] has been extended to show that the fields in the image

of symmetrical focussing reflectors can be generated by certain hybrid modes to provide theoretically aberrationless behavior[23]. An aperture source is described that uses a corrugated waveguide structure to generate a set of waves that combines to provide a theoretically high efficiency. Further developing his earlier ideas of spherical harmonic expansions, Ricardi has recently provided a technique for synthesis of the fields on a surface enclosing a transmitting feed[24]. This treatment for the transmitting feed synthesis provides for the solution to an electromagnetic boundary value problem, identifying as boundaries the reflector surface and the surface of a smaller sphere enclosing the feed region. It is with this technique, substantially different from those involving geometrical optics or approximations of stationary phase, offering a solution that appears to contain inherent accuracy, with which this thesis is concerned.

CHAPTER II

PROBLEM STATEMENT AND THE THEORY OF GEOMETRICAL OPTICS

2.1 The solution proposed by Ricardi to the problem of the spherical
     reflector microwave antenna relates two sets of electromagnetic fields
     over portions of surfaces of two concentric spheres. Due to the mathe-
     matical formulation of the problem, one surface coincides with that of
     the reflector while the other surface is taken at a radius of interest
     within that of the reflector. Origin of both spheres is at the center
     of curvature of the reflector (figure 2). The fields over the reflector
     surface are specified to be those fields that will produce a desired
     field distribution over the aperture of the reflector following reflection
     from its surface. The fields at the reflector surface are then expanded
     in a spherical wave expansion. Thus it may be determined that if the field
     distribution given by this expansion, evaluated at the inner surface, can
     be somehow generated by a source within this surface that the appropriate
     reflected fields will appear, as desired, over the aperture. Interpreta-
     tion of the fields at various radii has revealed that there are certain
     radii coincident with nearly constant phase fronts. Synthesis of these
     fields would be enhanced due to a potential lessening of the complexity
     of the radiating structure. Exactly which radius to be chosen for the
     inner surface is beyond the scope of this work, but is covered by
     Ricardi[25].

It is the hypothesis of this work that the technique of solution to the boundary-value problem may be applied to a reference sphere whose origin is a variable distance along the axis of symmetry and to the surface of which outgoing rays from a hypothetical feed located within this reference sphere would be traced if the spherical reflector were absent. The rays outgoing from the region of the hypothetical feed would be precisely those rays representing the fields that would, upon reaction with the surface of the spherical reflector, reflect a desired illumination over the reflector aperture. These rays would be based upon the rays reflecting from the spherical surface when illuminated by an incident plane wave over the aperture. Strictly speaking, this analysis begins with the principles of the receiving case, but then requires the field distribution to be produced over the reference sphere by some transmitting feed. It is then the reaction of the radiated field with the spherical reflector that theoretically produces a desired wavefront over the aperture. The geometry for this case is given by figure 3.

Thus, within the limits imposed on ray tracing technique by theory of geometrical optics, Ricardi's results for the transmitting feed case may be compared to an approximate solution that originates with the receiving situation. It is further possible that such a solution, known to be strictly valid only in the zero-wavelength limit, may yield results with less computation time than the exact solution within an appreciably small deviation in results. The choice of origin of the system of concentric spheres suggests that a more detailed analysis of
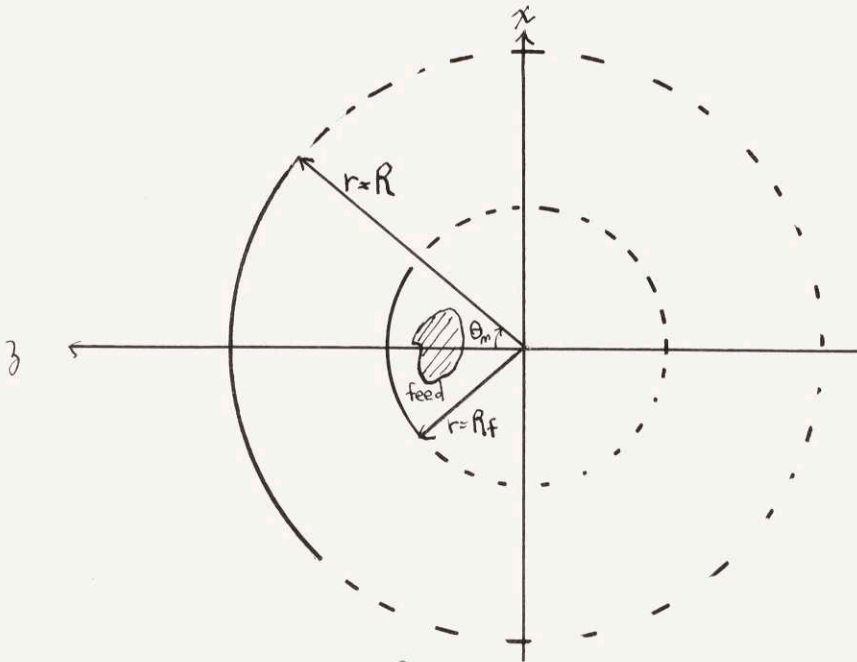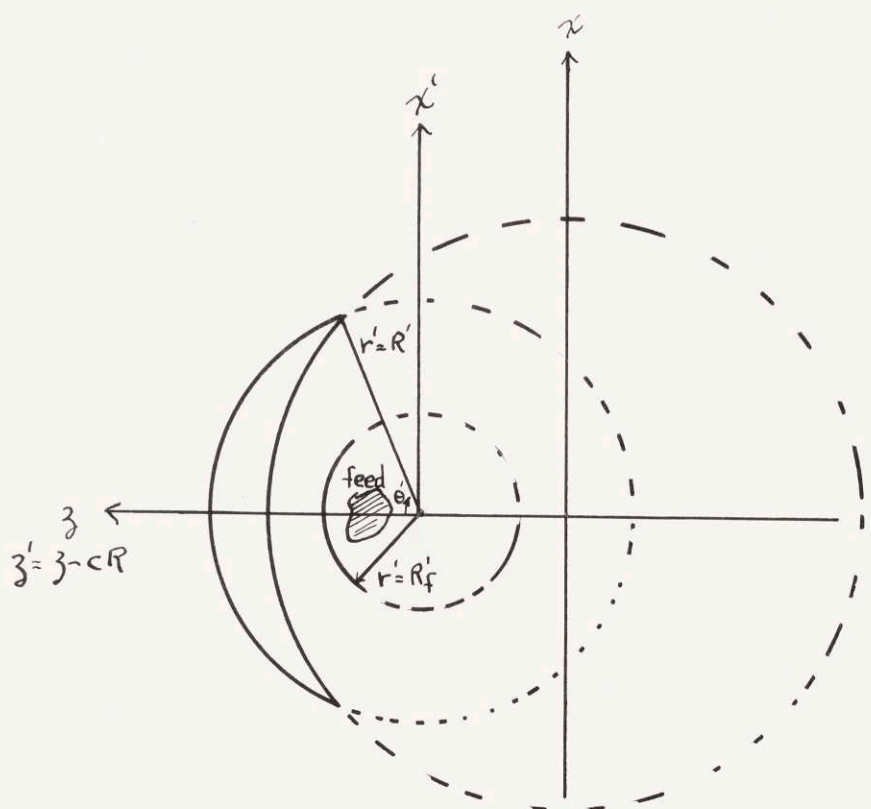
figure 2

figure 3

19

the fields in a particular region may be conducted in an economical fashion, since the fields will be distributed over a sphere of smaller radius than the previous problem's inner sphere with origin at that of the reflector.

We thus proceed to describe the illumination of a spherical reflector by a uniform plane wave to illustrate certain character-istics of the reflector. This is followed by development of geometrical optics principles essential to the description of the fields over the reference sphere. Finally, expressions will be developed that yield the amplitude, phase, and direction of the electric field over the reference sphere.

2.2   It has been noted previously that rays reflected from the spher-ical surface following illumination by a uniform plane wave over the aperture cross the axis of symmetry at varying distances from the paraxial focus. This phenomenon may be analytically formulated to illustrate the generation of caustic surfaces by these reflected rays. In fact, it will be shown that the caustic surface is the envelope of reflected rays. Consider the situation given by figure 4.

figure 4
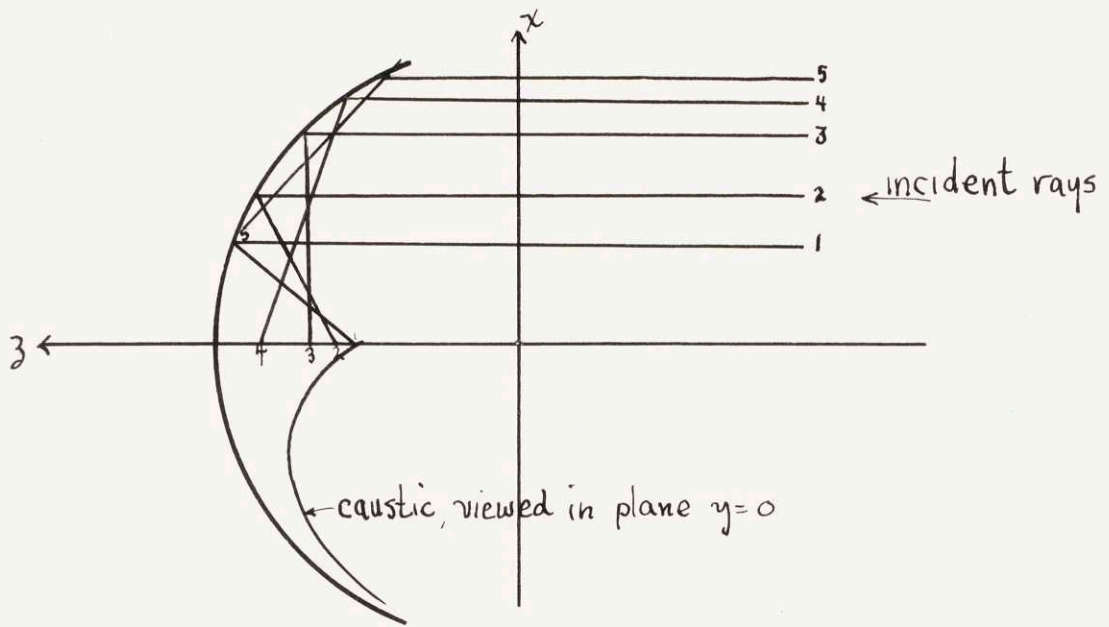
Constrained only by the fact that the angles of reflection and incidence
are identical, the equations of rays may be given by the slope intercept
form of the straight line equation. That the rays are straight lines and
the angles equal will be covered in detail in later sections. Viewing
the system in the x-z plane we have:

$$\frac{x - x_0}{z - z_0} = \tan 2\theta \qquad (2.1)$$

Points on the reflector surface are given by:

$$x = R \sin\theta$$

$$z = R \cos\theta$$

Letting points on the envelope be x_c, z_c, and substituting into 2.1:

$$x_c = R \sin\theta - (R \cos\theta - z_c)\tan 2\theta \qquad (2.2)$$

Thus points on the caustic surface as viewed in the x-z plane become functions of parameter θ. We then form the function $f(x,z,\theta) = 0$ that will be satisfied by points on the caustic.

$$f(x,z,\theta) = x_c - R \sin\theta + (R \cos\theta - z_c)\tan 2\theta = 0 \qquad (2.3)$$

Adjacent points on the caustic generated by rays incident at angle $\theta + \delta\theta$ will still satisfy the function for small $\delta\theta$. Since both functions $f(x_c, z_c, \theta)$ and $f(x_c, z_c, \theta+\delta\theta)$ are equal to zero, their difference as well is equal to zero. We can then form the expression valid in the limit of small $\delta\theta$:

$$\lim_{\delta\theta\to 0} \frac{f(x_c, z_c, \theta+\delta\theta) - f(x_c, z_c, \theta)}{\delta\theta} = 0$$

or

$$\frac{d\, f(x_c, z_c, \theta)}{d\theta} = 0 \qquad (2.4)$$

Differentiating and solving for z_c yields:

$$z_c = \frac{R}{2} (2 \sin^2\theta + 1)\cos\theta \qquad (2.5)$$

This expression for z_c is then substituted into 2.2 to solve for x_c.
Manipulation with trigonometric identities yields the parametric form
of the equations for the caustic surface:

$$x_c = R \sin\theta = \frac{R}{4}(3 \sin\theta - \sin 3\theta) \qquad (2.6)$$

$$z_c = \frac{R}{2}\cos (2 \sin^2\theta + 1) = \frac{R}{4}(3 \cos\theta - \cos 3\theta) \quad (2.7)$$

Thus it has been shown that the reflected rays' envelope forms the
caustic surface and quantitative expressions for this surface have been
developed. They will be called upon in conjunction with development of
the expression for amplitude.

2.3   Electromagnetic field problems may be formulated in two contrasting
fashions, following from a choice of application of the Maxwell field
equations. In one treatment, relationships may be derived that determine
what fields will arise from a prescribed set of sources. The field and
vector Helmholtz equations are integrated by application of a vector
Green's theorem, and express the fields at an observation point as the
sum of contributions from the sources distributed throughout a particular
volume and from fields on the surface of the volume arising from sources
outside the volume.[26] This rigorous treatment indicates that the field
represents a flow of energy outward from the region of the sources, and

23

that these sources and fields satisfy certain assumptions of continuity over the surface of interest, as required by application of the Green's theorem. In the second treatment, the integral relations derived by the first method may be applied to yield expressions for the field vectors at a specified point, given the values of the fields over a surrounding equiphase surface, or wavefront, without direct reference to the sources generating the wavefronts[27]. These integral expressions are the analytic formulation of the Huygens-Fresnel principle, which states that each point on the equiphase surface can be regarded as a secondary source of electric and magnetic current and charge which in turn gives rise to a spherical wavelet. The fields at a point of interest may be obtained by a superposition of these wavelets, considering the phase difference upon arrival at the point of interest. Hence, energy flow is a wave phenomenon—one which may be studied without reference to the sources of energy. As before, the rigor of the solution depends upon adherence of the given field distribution to several constraints as imposed by application of the Green's theorem.

While the Huygens-Fresnel relation provides expressions for solutions to the wave equation that satisfy Maxwell's equations, complexities of integration of these expressions often render solutions impractical, or require approximations to be made that eventually lessen the rigor of the solution only after substantial manipulation. In these cases it becomes convenient to approach the propagation of waves from the standpoint of geometrical optics, wherein a rigorous solution is sacrificed for a

simpler formulation that offers a more immediate solution, subject to several additional constraints on the problem. In geometrical optics, successive positions of equiphase wavefronts of the fields and an associated system of rays are related.

In an arbitrary medium the wave field is characterized by both a ray velocity and wave velocity at every point, where the ray velocity is the velocity of energy propagation, directed as the ray passing through the point of interest, and the wave velocity is the rate of displacement of the wavefront in the direction normal to the surface. The energy propagates at the speed of light in vacuum, c. The wavefront propagates at the velocity v, a function of the medium.

We proceed to describe the relations among wavefront and phase, considering wavefronts generated by some source propagating in a steady-state radiation. Let the wavefront at time t_o be the surface $L(x,y,z)=L_o$, a surface of constant phase $\Psi = (\omega/c)L_o$ relative to some point. The wavefront at some short time δt later is the surface $L(x,y,z) = L_o + \delta L$. The phase difference between successive wavefronts is then given by $(\omega/c)\delta L$. Since the wave proceeds from one surface to the next in time δt while the phase at any fixed position changes at the rate ω, this phase difference must be equal to $\omega\delta t$. Further, if δ_{sn} is the distance between the adjacent surfaces and if v is the wave velocity, then $v\delta t = \delta_{sn}$.

We then relate these expressions:

$$(\omega/c)\delta L = \omega\delta t = (\omega\delta_{sn})/v$$

or
$$\delta L/\delta_{sn} = c/v = \eta \text{ , index of refraction of the medium} \quad (2.8)$$

Note that expression 2.8 is the directional derivative of a scalar L in the direction of the normal to the wavefront. By definition of the directional derivative of a scalar function ϕ,[28]

$$d\phi/ds = T\cdot\nabla\phi$$

where T is the unit vector indicating direction in which the derivative is taken. By definition of the vector dot product, with Θ the angle between T and $\nabla\phi$,

$$d\phi/ds = T\cdot\nabla\phi = |T||\nabla\phi| \cos\Theta = |\nabla\phi|\cos\Theta$$

For our case the direction of interest in normal to the front, and $\Theta = 0$. Hence:

$$\delta L/\delta_{sn} = |\nabla L| = c/v = \eta \quad (2.9)$$

Considering the curvature of rays in an inhomogeneous medium we can demonstrate that the rays are rectilinear in a homogeneous medium. Let S be a unit vector in the direction of a ray at the point of interest. This vector is normal to the wavefront and has the direction of ∇L. Then,

$$|\nabla L| = \eta \quad or \quad |\nabla L| / \eta = 1$$

Then
$$S = \nabla L / \eta \tag{2.10}$$

Let N be a unit vector in the direction of the radius of curvature of the ray at the same point of interest and ρ the radius of curvature of the ray at the point. The vector curvature is defined[29] as N/ρ . This vector curvature is also given by dS/ds, where s is a distance measured along the ray. By definition and vector identity the following expansion can be made:

$$dS/ds = (S \cdot \nabla)S = - S \times (\nabla \times S) = N/\rho \tag{2.11}$$

This expression can be manipulated to show a simple relationship between curvature of the rays and index of refraction of the medium. Details are left to appendix 1. The result of interest is:

$$1/\rho = N \cdot \nabla(\ln \eta) \tag{2.12}$$

Thus for a homogeneous medium where the index of refraction is constant, or independent of position, we see that the right hand side of 1.12 is zero, indicating that the radius of curvature of the ray is infinite, indicating that the rays are, in fact, rectilinear. It follows that $\nabla XS = 0$, which is a sufficient condition for the existence of a family of surfaces orthogonal to a field of vectors S.

The relationship of the amplitude of fields on successive wavefronts can be determined from the premise of geometrical optics that rays are lines of flow energy and that no power flows across the sides of a tube of rays. These results were verified in the preceeding paragraph. Silver[30] considers two surfaces of waves L_1 and L_2 and a tube of rays that cuts out elements of area dA_1 and dA_2 on the respective surfaces. By conservation of energy requirements, the flow across any section normal to the tube will be constant. In terms of the Poynting vector defined by

$$S = \tfrac{1}{2}(EXH^*)$$

we can formulate the flow constraint by

$$S_1 \ dA_1 = S_2 \ dA_2$$

Since in free space the Poynting vector is proportional to the magnitude squared of the field, between successive wavefronts the following relation will hold:

$$|E_1|^2 dA_1 = |E_2|^2 dA_2 \qquad (2.13)$$

Considering the ray through point A on the surface L_1 coincident with the z-axis in figure 5, let the xz,yz planes coincide with the principle planes of L_1 at A. A ray through an adjacent point B lying in L_1 and the x-z plane will intersect the ray through A at the point O_x, a distance R_1 away. This distance R_1 thus is one of the principle radii of L_1 at A. A similar analysis reveals the definition of the other radii R_2 based upon intersection of rays passing through adjacent points in the x-y plane. The point A' on L_2 lies on the ray through point A. At A' local coordinates x', y' are constructed. Since the fronts are spaced apart by the distance P, the two principle radii of curvature of the wavefront L_2 at the point A' are $R_1 + P$ and $R_2 + P$.

Considering the elements of area dA_1 and dA_2 around the points A, A' bound by the curve C, C' on surfaces L_1 and L_2 respectively, we can write:

$$dA_1 = \int_C (xdy-ydx)$$
$$dA_2 = \int_{C'} (x'dy'-y'dx') \qquad (2.14)$$

From inspection of figure 5, and by the law of sines we can relate various distances:
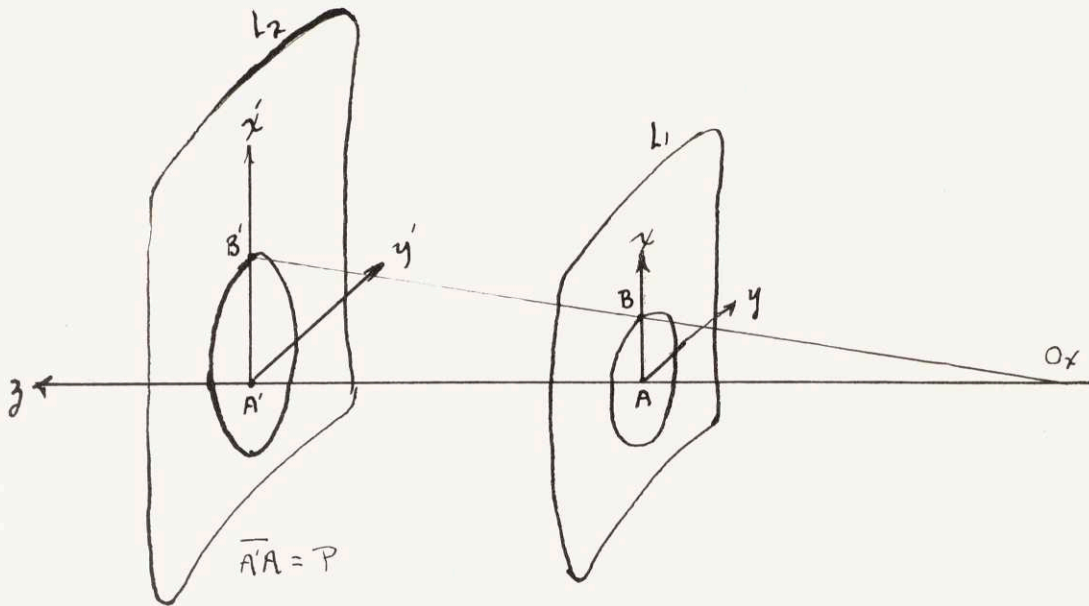
figure 5

$$x' = \frac{(R_1 + P)x}{R_1} \qquad\qquad y' = \frac{(R_2 + P)y}{R_2} \qquad\qquad (2.15)$$

By relating dx, dx', dy, dy' and substituting into 1.14 we obtain a relationship between the area elements:

$$dA_2 = dA_1 \frac{(R_1 + P)(R_2 + P)}{R_1 R_2} \qquad\qquad (2.16)$$

Substitution of 2.16 into 2.13 we obtain:

$$|E_1|^2 dA_1 = |E_2|^2 dA_1 \frac{(R_1 + P)(R_2 + P)}{R_1 R_2}$$

For the case of a wavefront diverging from a region of sources this expression relates the amplitude at the wavefront farther from the source:

30

$$E_2 = E_1 \left| \frac{R_1 R_2}{(R_1 + P)(R_2 + P)} \right|^{\frac{1}{2}} \tag{2.17}$$

From the preceeding development it would appear that geometrical optics is based on the local behavior of the wavefront as a plane wave. Indeed, this is the basic tenet of the theory. The plane wave solution to the wave equation may be used to show that in the limit of decreasing wavelength the geometrical optics solution satisfies the Maxwell fields equations. The vector solutions appropriate to describe linearly polarized electromagnetic fields that behave locally like plane waves have the form:

$$E = A(x,y,z) \; e^{j(\omega t - k_o L(x,y,z))}$$

$$\tag{2.18}$$

$$H = B(x,y,z) \; e^{j(\omega t - k_o L(x,y,z))}$$

The amplitude vectors may be complex, but phases must be independent of position to fit the plane wave solutions. Substituting these forms of solution into the homogeneous forms of Maxwell's equations given by

$$\nabla \times E + j\omega\mu H = 0$$

$$\tag{2.19}$$

$$-j\omega\varepsilon E + \nabla \times H = 0$$

and expanding the resulting expressions, these may be solved for the
vector amplitudes A and B :

$$A = \frac{-k_o}{\omega\epsilon}(\nabla L \times B) + \frac{1}{j\omega\epsilon}(\nabla \times B)$$

$$B = \frac{k_o}{\omega\mu}(\nabla L \times A) - \frac{1}{j\omega\mu}(\nabla \times A)$$

(2.20)

where k_o is the free space propagation constant, $k_o = \omega\sqrt{\mu_o\epsilon_o}$.
Equations 2.20 may be solved to yield an expression in terms of A alone.
Using the definition of k_o and the index of refraction

$$\eta = c/v = (\epsilon\mu/\epsilon_o\mu_o)^{\frac{1}{2}}$$

we obtain the following expression:

$$A = \frac{-1}{\eta^2}(\nabla L \times \nabla L \times A) + \frac{1}{jk_o\eta^2}(\nabla L \times \nabla \times A + \nabla \times \nabla L \times A) +$$

$$\frac{1}{\eta^2 k_o^2}(\nabla \times \nabla \times A)$$

(2.21)

Expanding 2.21 with the vector identity

$$\nabla L \times \nabla L \times A = L(\nabla L \cdot A) - A(\nabla L \cdot \nabla L)$$

we obtain for A :

32

$$A = \frac{-1}{\eta^2} \{ \nabla L(A \cdot \nabla L) - A|\nabla L|^2 \} + \frac{1}{jk_0 \eta^2} (\nabla L \times \nabla \times A + \nabla \times \nabla L \times A)$$

$$+ \frac{1}{\eta^2 k_0^2} \nabla \times \nabla \times A \qquad\qquad (2.22)$$

A similar expression results for B, replacing A with B in 2.22. If L and the first and second derivatives of A and B are finite, the last two terms of 2.22 are of the order $1/k_0$ and $1/k_0$ compared to the first term. As the wavelength approaches zero, k_0 approaches infinity, and we are left with the following expressions:

$$A = \frac{-1}{\eta^2} \{ \nabla L(A \cdot \nabla L) - A|\nabla L|^2 \}$$

$$(2.23)$$

$$B = \frac{-1}{\eta^2} \{ \nabla L(B \cdot \nabla L) - B|\nabla L|^2 \}$$

For these expressions to yield identity of amplitude of the vectors A and B we see that the following must be true for the zero wavelength case:

$$A \cdot \nabla L = 0$$

$$B \cdot \nabla L = 0$$

These two conditions note that A and B are transverse to the gradient of L, or that they both lie in a plane transverse to the direction of propagation. Furthermore, since 2.20 expresses B in terms of A we have:

$$B = \sqrt{\epsilon/\mu}\{ \frac{(\nabla L}{\eta} \times A) - \frac{1}{jk_o \eta} \nabla \times A \} \qquad (2.24)$$

We see that in the zero wavelength case the second term vanishes
and we are left with an expression that implies vector amplitude B is
perpendicular to A as well as transverse to the direction of propagation,
since $\nabla L/\eta$ is a unit vector in the direction of propagation.

Thus the field vectors of geometrical optics possess the properties
of plane waves in what might be called the far-zone fields, indicating
great distances from the source with respect to wavelength. The condition
for neglecting terms of the order $1/k_o$ and $1/k_o$ for short wavelengths
require that all associated derivatives are finite. In the neighborhood
of geometrical focal points or caustic surfaces, the function L varies
rapidly, and geometrical optics predicts infinite amplitudes , which
must be rejected on non-physical grounds. At the region of geometrical
shadow the approximations begin to predict erroneous results due to
the rapid variation of amplitude over distances small compared to
wavelength. In these regions the simple methods do not work, and dif-
fraction and scattering theory must be used.

Further work [31] has determined that the Huygens-Fresnel relation in
the zero-wavelength case approaches the point-to-point amplitude relation-
ship predicted by the geometrical optics concept of energy flow in tubes
of rays. Agreement holds in the far-zone approximation, at distances
greater than wavelength, and reveals the constraint on amplitude

A's normal derivative that, besides being finite everywhere,

$$\frac{1}{A} \frac{\partial A}{\partial n} << \frac{2\pi}{\lambda}$$

This is satisfied in the limit of zero wavelength providing the fractional change in amplitude over distance equal to that of a wavelength is small compared with unity.

Since the basic tenet of geometrical optics requires that the wavefront behave locally like an infinite plane wave, scattering phenomenon may be interpreted geometrically, and appropriate laws of reflection derived from the field equations and boundary conditions. That these results are valid can be developed from other principles of optics[32] including Fermat's principle and the law of the optical path, demonstrating the properties of optical rays and the reflection phenomenon, or Snell's laws.

We consider the two-dimensional analysis of an infinite plane wave incident upon an infinitely conducting (that is to say perfectly reflecting) sheet. The geometry of the problem is described by figure 6.
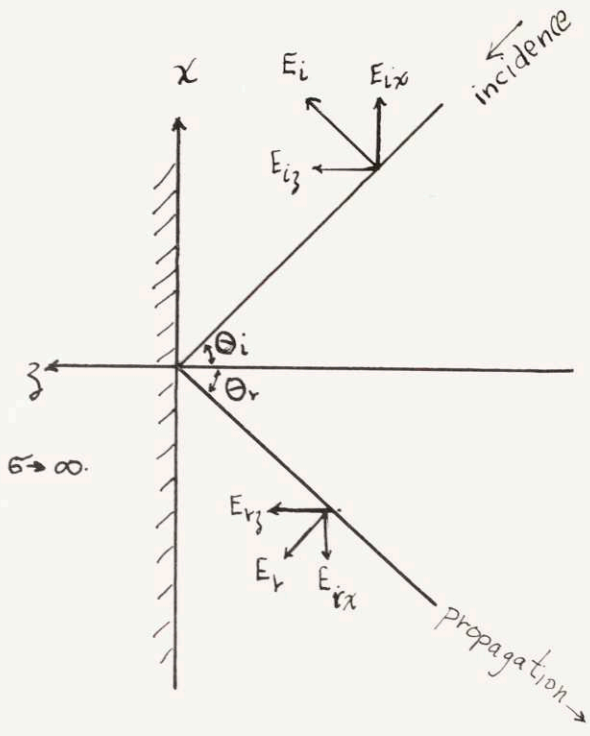
figure 6

The incident fields will have the form:

$$H_i = i_y \, h_i \, e^{-jk_o z \cos\theta_i + jk_o x \sin\theta_i}$$

$$(2.25)$$

$$E_i = \zeta(i_x \, h_i \cos\theta_i + i_z \, h_i \sin\theta_i) \, e^{-jk_o z \cos\theta_i + jk_o x \sin\theta_i}$$

where ζ is the wave impedance of free space, equal to $(\mu_e / \varepsilon_e)^{\frac{1}{2}}$

The reflected fields will have the following form:

$$H_r = i_y \, h_r \, e^{+jk_o z \cos\theta_r + jk_o x \sin\theta_r}$$

$$(2.26)$$

$$E_r = \zeta(-i_x \, h_r \cos\theta_r + i_z \, h_r \sin\theta_r) e^{+jk_o z \cos\theta_r + jk_o x \sin\theta_r}$$

Since at $z = 0$ for all x and y the boundary condition on the tangential component of electric field requires that $(E_i + E_r)_{tang} = 0$. Then, equating reflected and incident fields appropriately we obtain:

$$\Theta_i = \Theta_r$$

$$h_i = h_r$$

$$e_i = e_r$$

Thus we note that the following boundary conditions exist at the interface:

$$(E_i + E_r)_{tang} = 0$$
$$(E_i)_{nor} = (E_r)_{nor} \qquad (2.27)$$

These expressions may be given in terms of a vector relationship:

$$n \times (E_i + E_r) = \theta$$
$$n \cdot E_i = n \cdot E_r \qquad (2.28)$$

We can examine this vector relationship to determine an expression for the field reflected from a surface in terms of the incident field and the surface normal- assuming that the field acts locally as a plane wave.

37

With the vector form of the boundary conditions we form the cross product
of the normal $\vec{n}$ and the first expression of 2.28. We then multiply the
second of 2.28 with the normal vector $\vec{n}$ and add the two expressions.
This yields:

$$n \times E_r \times n + (n \cdot E_r)n = -n \times E_i \times n + (n \cdot E_i)n$$

Expanding by the vector identity

$$A \times B \times C = (A \cdot C)B - (A \cdot B)C$$

we obtain the expression

$$E_r = -E_i + 2(n \cdot E_i)n \qquad\qquad (2.29)$$

This may be interpreted to express quantitatively the fact that the
reflected field experiences reversal of its sense of tangential
components in order to provide a zero tangential field at the surface
of the reflector.

Thus we have demonstrated that the approximate methods of geometrical
optics involving point-to-point transformations along rectilinear rays
between successive wavefronts or surfaces of constant phase can provide

adequate phase and amplitude information providing certain constraints
are observed. Furthermore, that these fields satisfy Maxwell's fields
equations and the wave equation within the limits of certain constraints
has been demonstrated by a zero-wavelength limit. We summarize the results
of geometrical optics in which we are interested as relevant to this work:

1. Energy passing through consecutive cross-
   sections of a tube of neighboring rays is
   constant.

2. Rays in a homogeneous medium are rectilinear.

3. At a surface of reflection, an incident
   wavefront behaves locally like a plane
   wave, and the reflection of rays may be
   geometrically interpreted in accordance
   with specular reflection laws.

The following constraints must be observed for the geometrical optics
approximations to hold:

1. All lengths of interest, radii of curvature,
   for example, must be large compared to a
   wavelength.

2. Spacing between neighboring rays must
   change very little over distances on the
   order of wavelength.

3. The fractional change in amplitude of
   field quantities over distances on the
   order of wavelength must be small com-
   pared to unity.

4. Geometrical optics cannot be used in
   the region of geometrical shadow.

5. Geometrical optics fails at focal points
   or caustic surfaces, predicting non-
   physical results.

2.4 It remains to utilize the previously developed expressions to describe

the phase, amplitude and direction of the electric field over the ref-

erence sphere. The choice of radius of the reference sphere is discussed,

as is the technique of ray tracing to be used. Expressions for phase

and amplitude on the reference sphere are developed, relating these

quantities to those incident upon the reflector surface. Finally, the

distribution over the reference sphere is related to a coordinate system

with coincident origin.

For the geometry of figure 7, we consider determination of the fields

produced by some source, directed towards the reflector, that will produce

illumination over the aperture in the form of waves propagating in the

− z direction. The fields propagating in this direction will be of the

form:

$$E, H \propto e^{jk_o z}$$

or in spherical coordinates:

$$E, H \propto e^{jk_o R \cos\Theta}$$

Since we desire to specify these fields over a reference sphere of radius

R' with origin at z = cR, where c is some constant fixing the origin,

the phase expression must be corrected to account for the additional

figure 7

Labels in figure 7:
- x (vertical axis)
- ray 1
- L_1
- reflected ray 2 traced back to reference sphere
- L_2
- ray 2
- 2
- $\Theta = \Theta_c \uparrow$
- z (horizontal axis)

figure 8

Labels in figure 8:
- x (vertical axis)
- incident ray
- (x_a, z_a)
- A
- (x_m, z_m)
- M
- $r = R$
- $r' = R'$
- $z = cR$
- Θ_m
- z (horizontal axis)
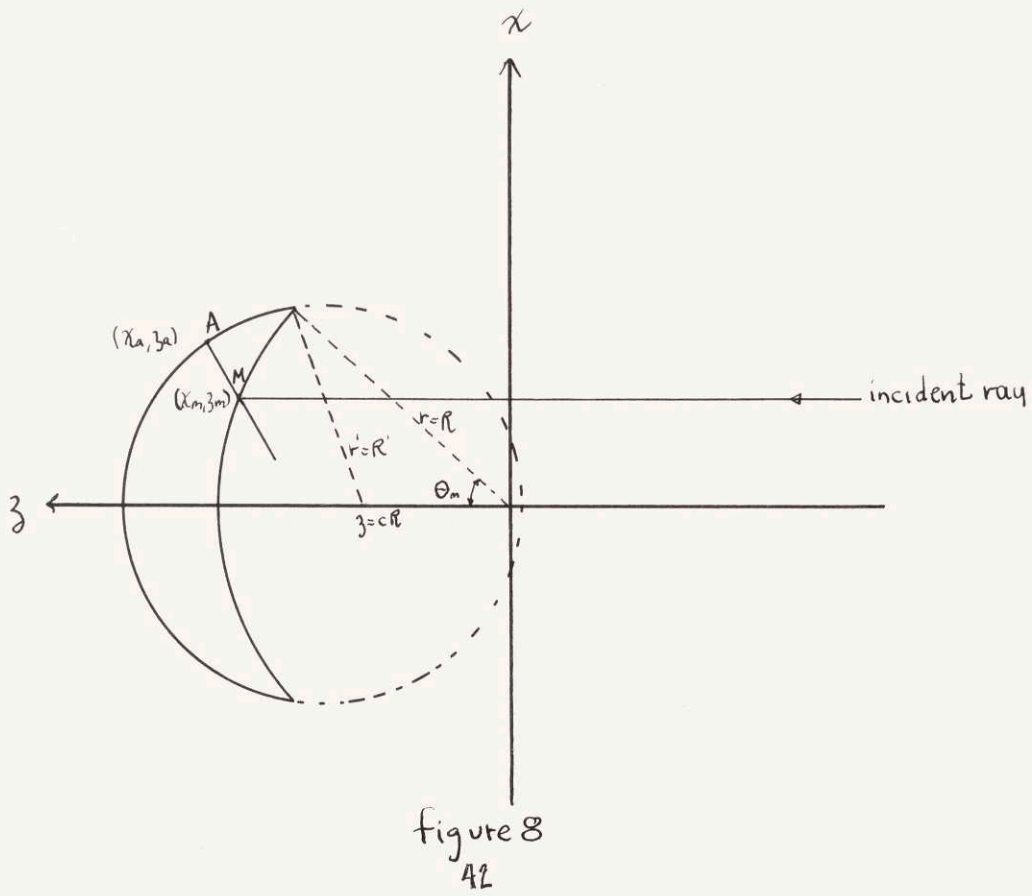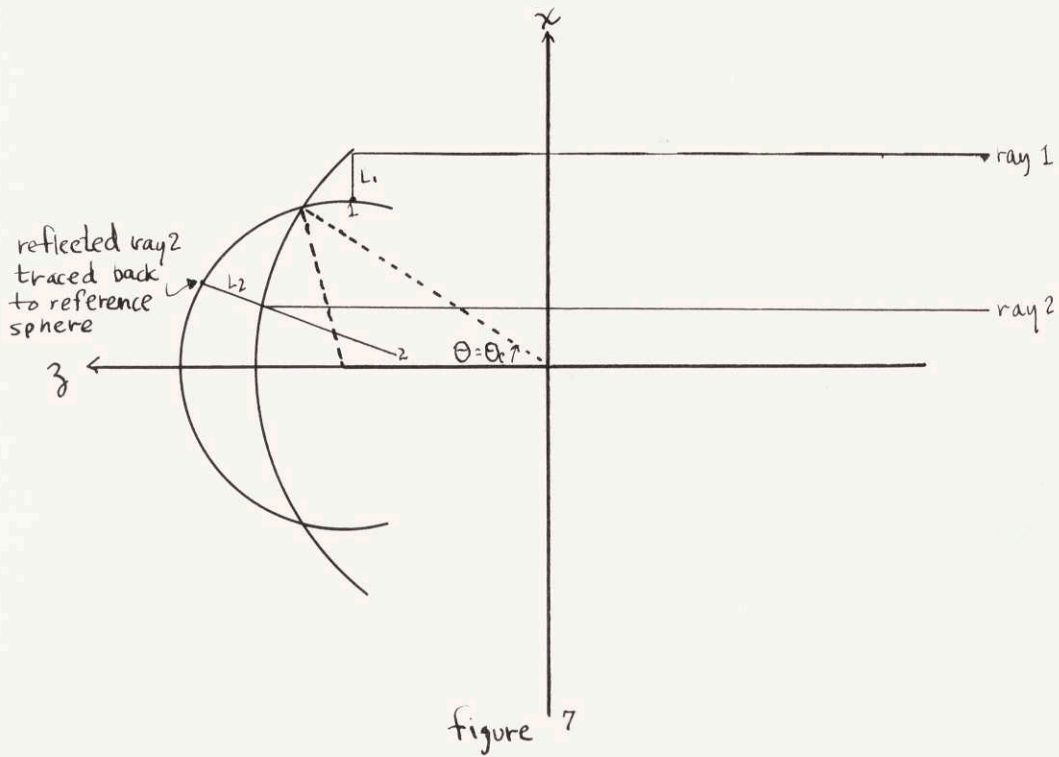
path length of travel to the reference sphere. Inspection of figure 7 indicates that the phase variation has two cases of interest, one for angles $\theta > \theta_c$ and the other for the case of $\theta < \theta_c$, where θ_c is the angle at which the reference sphere intersects the spherical reflector. The variation in field expressions is introduced as:

$$\theta > \theta_c \qquad E,H \quad \propto \quad e^{jk_o (Rcos + L_1)}$$

$$(2.30)$$

$$\theta < \theta_c \qquad E,H \quad \propto \quad e^{jk_o (Rcos - L_2)}$$

Inspection of the exponent suggests that if appropriate values of other parameters could be found so as to keep the difference to a minimum that synthesis might be enhanced, since the smaller exponent represents a slower varying sinusoid. Furthermore, amplitude considerations in the geometrical optics approximation, namely the desire to avoid the region of the caustic surface, suggest that a wise choice would be to consider the reference sphere intersecting the reflector surface at the latter's extreme edge. Thus the radius of the reference sphere will be constrained by the radius of the reflector under investigation, R, the position of the origin of the reference sphere $z = cR$, and the maximum angle subtended by the reflector. By laws of trigonometry we observe:

$$R'^2 = R^2 + c^2R^2 - 2cR^2cos\theta_m \qquad (2.31)$$

The ray tracing technique proceeds from a ray incident upon the reflector at a particular angle of interest. The ray reflects in accordance with the previously developed laws of reflection. We then assume that if a hypothetical source could produce the appropriate fields that would give the same illumination as we have upon the aperture, these rays would remain as we have determined, but the sense of propagation of energy along the rays would be reversed. We then remove the reflector, and trace the rays until they intersect the reference sphere. Within the limits of geometrical optics, we can estimate the amplitude and phase at each point of intersection, based upon the extra path length travelled by the waves, along the rays, to the reference sphere.

It is necessary to calculate the distance L. We proceed with an equation determining the distance between points on the reflector and points on the reference sphere, as measured along the ray of interest. Referring to figure 8:

$$L^2 = (x_a - x_m)^2 + (y_a - y_m)^2 + (z_a - z_m)^2 \qquad (2.32)$$

where

$$x_a = R' \sin\theta' \cos\phi' \qquad x_m = R \sin\theta \cos\phi$$

$$y_a = R' \sin\theta' \sin\phi' \qquad y_m = R \sin\theta \sin\phi$$

$$z_a = R' \cos\theta' + cR \qquad z_m = R \cos\theta$$

44

Noting from symmetry that $\phi = \phi'$, and substituting, expanding terms we obtain:

$$(2.33) \qquad L = \sqrt{(R'\sin\theta' - R\sin\theta)^2 + (R'\cos\theta' + cR - R\cos\theta)^2}$$

To proceed, we must relate θ and θ' . Viewing in the x-z plane, the equation of ray is given by:

$$
\begin{aligned}
x &= (z - z_o)\tan 2\theta \\
y &= 0
\end{aligned}
\qquad (2.34)
$$

From the equation of a spherical surface :

$$R'^2 = x^2 + (z - cR)^2 + y^2 \qquad (2.35)$$

We can solve 2.34 and 2.35 in the plane $y = 0$ to yield an expression representing the intersection of a ray and the surface of the reference sphere. Solving for z_o, intercept of the z-axis we obtain:

$$\frac{R}{\sin(\pi - 2\theta)} = \frac{z_o}{\sin\theta} \qquad (2.36)$$

Substituting 2.34 into 2.35, and expanding in a straightforward fashion we obtain, with substitution of 2.36:

$$z^2 - 2z(R\sin\theta\sin2\theta + cR\cos^2 2\theta) + R^2\sin^2\theta - \cos^2 2\theta(R'^2 - c^2 R^2) = 0$$

Details of the manipulation are included in appendix 1. Normalizing all distances to R, radius of the reflector under investigation, we obtain:

$$z_n^2 - 2z_n(\sin\theta\sin2\theta + c\cos^2 2\theta) + \sin^2\theta - \cos^2 2\theta(R_n'^2 - c^2) = 0 \tag{2.37}$$

where

$$R_n' = \frac{R'}{R} \qquad\qquad z_n = \frac{z}{R}$$

Solving the quadratic 2.37 by usual methods, we obtain for z_n :

$$z_n = (\sin\theta\sin2\theta + c\cos^2 2\theta) +$$

$$\sqrt{(\sin\theta\sin2\theta + c\cos^2 2\theta) - \sin^2\theta + \cos^2 2\theta(R_n'^2 - c^2)} \tag{2.38}$$

Noting from the geometry of figure 8:

$$R'\cos{}' = z' = z - cR$$

or

$$\cos\theta' = \frac{(z - cR)}{R'} = \frac{(z_n - c)}{R_n'} \tag{2.39}$$

Substituting equation 2.38 into 2.39 the following relationship between angles θ and θ' is obtained:

$$\cos\theta' = \frac{1}{R_n'} (\sin\theta\sin2\theta + c \cos^2 2\theta - c$$

$$+ \sqrt{(\sin\theta\sin2\theta + c \cos^2 2\theta) - \sin^2\theta + \cos^2 2\theta(R_n'^2 - c^2)} \quad)$$

$$(2.40)$$

Equation 2.40 states that there is a relationship between angles such that for every angle of incidence on the reflector surface there exists an angle θ', as measured from the origin of the reference sphere, that describes the intersection of the reflected ray traced back to the reference sphere and the surface of this sphere. Thus the angles may be related in terms of the parameters of the reflector under investigation, R and θ_m , and the center of the reference sphere implied by the value of c. Once the angles associated with a particular incident ray have been related, they may be substituted into 2.33 to yield the distance L as a function of the point of interest on the reference sphere.

Equation 2.17 was developed to express the amplitude of field quantities on one wavefront with respect to the field quantities on another front. It is seen that the amplitude varies with the two principle radii of the wavefront and the distance of separation between fronts. It is necessary, then, to develop expressions for the radii.
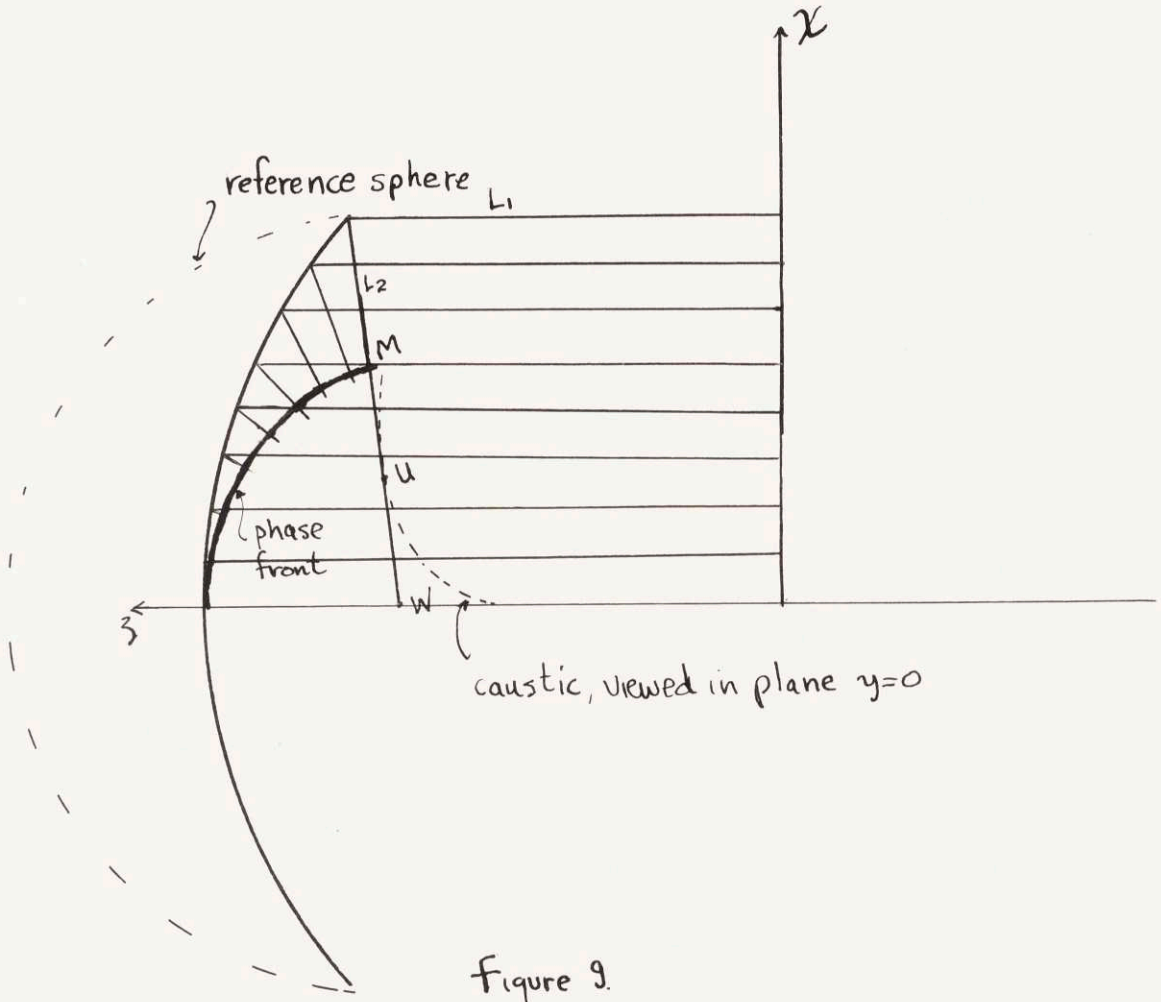
47

Figure 9.

caustic, viewed in plane $y=0$

Once again we consider the case of a spherical reflector illuminated by an incoming plane wave. A typical reflected wavefront has been constructed in figure 9, where the front represents a surface of constant phase as defined by the total path length measured along each ray, $L_1 + L_2 = R$. The wavefront is formed by connecting normals erected on each ray at the point where total path length equals the radius of the reflector. Figure 9 shows the front as viewed in the plane $y = 0$. From symmetry, it may be seen that the surface of the front can be generated by revolution of the projection in figure 9 around the axis.

At any point of interest, a wavefront may be passed through this point by choice of the appropriate path length. At each point the wavefront will have two principle radii of curvature. Since a ray is normal to the front and any two adjacent rays intersect at the caustic surface, forming the envelope that is the caustic surface, it is seen that one radius of interest is the distance from the front at the point of interest to the point on the caustic, as measured along the ray. The second radius of curvature may be determined from the axial symmetry of the system. In the ϕ direction, adjacent rays will intersect at the axis of symmetry, and the second radius of curvature will be the distance from the front at the point of interest to the axis, measured along the ray.

Rays incident upon the reflector at an angle θ are reflected at this angle, pass tangent to the caustic surface and cross the axis. The coordinates of the point to which tangency occurs are given by equations 2.6 and 2.7, the parametric equations of the caustic. From figure 9 we see:

$$R_1 = MU = \sqrt{(z_m - z_c)^2 + (x_m - x_c)^2} \qquad (2.41)$$

$$R_2 = MW = \sqrt{(z_m - z_o)^2 + (x_m - 0)^2} \qquad (2.42)$$

where
$$z_m = R\cos\theta$$

$$x_m = R\sin\theta$$

$$z_o = R \frac{\sin\theta}{\sin2\theta}$$

Substituting into equations 2.41 and 2.42, and normalizing all quantities to the radius R we obtain:

$$R_{1n} = \frac{\cos\theta}{2} \qquad (2.43)$$

$$R_{2n} = \frac{1}{2\cos\theta} \qquad (2.44)$$

Details of the manipulation involved are covered in appendix 1.

Although the wavefront has been analyzed by considering illumination of the reflector by an incoming wave, it is the fact that if a source can be provided that can generate such a wavefront as has been described, the wavefront will be reflected from the spherical surface to yield an outgoing plane wave over the reflector aperture. Figure 9 represents a graphical illustration of the method of compensation suggested by Ashmead and Pippard,[33] a wavefront whose departure from sphericity is just that needed to transform into a plane wave upon reflection.

Since we wish to describe the fields over the reference sphere as a function of coordinates with origin at that of the reference sphere, we must introduce a transformation of the field vectors. Initially, field quantities were described upon incidence in terms of coordinates with origin at that of the reflector. The geometry of interest is described in figures 10 and 11, considering both cases where the center of curvature of the reference sphere is exterior and interior to the intersection of the reflected marginal ray (edge of reflector being the point of incidence) and the axis. Note that due to axial symmetry there is no modification necessary to the ϕ component. By inspection:

$$i_{r'} = i_r \cos (\theta' - \theta) + i_\theta \sin (\theta' - \theta)$$

$$(2.45)$$

$$i_{\theta'} = - i_r \sin (\theta' - \theta) + i_\theta \cos(\theta' - \theta)$$

x

$i_{\theta'}$

i_θ

i_r'

i_r

i_r

incident ray

ζ

figure 10

i_r'

$\angle = \theta' - \theta$

$i_\oplus$

i_r θ'

θ

$i_{\theta'}$

detail

x

i_r'

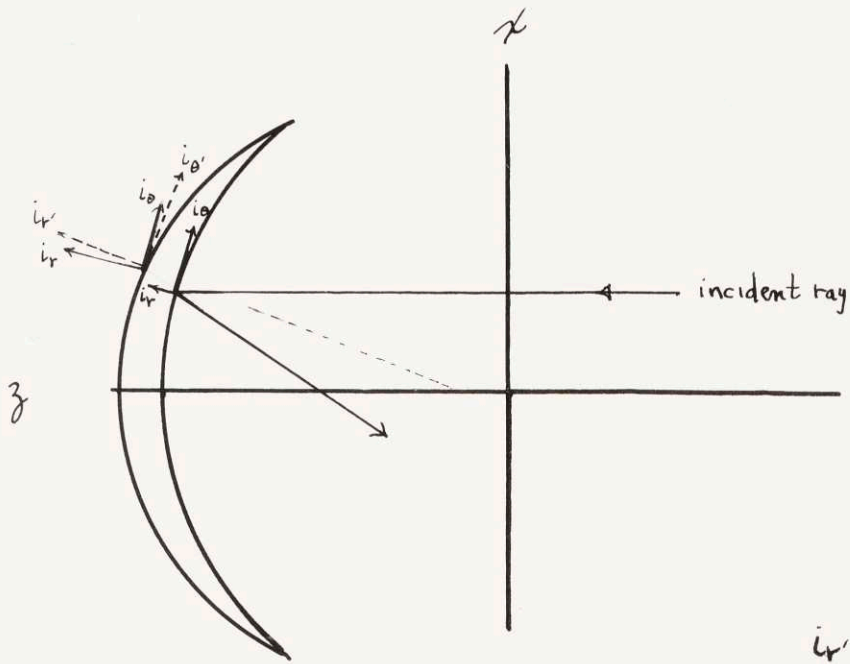i_θ

$i_{\theta'}$

i_r

i_θ

i_r

incident ray

ζ
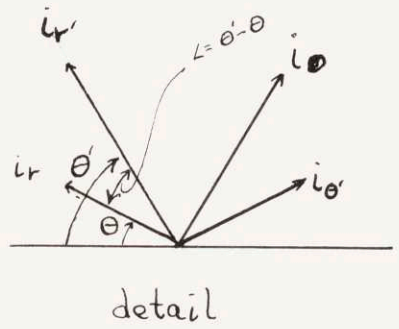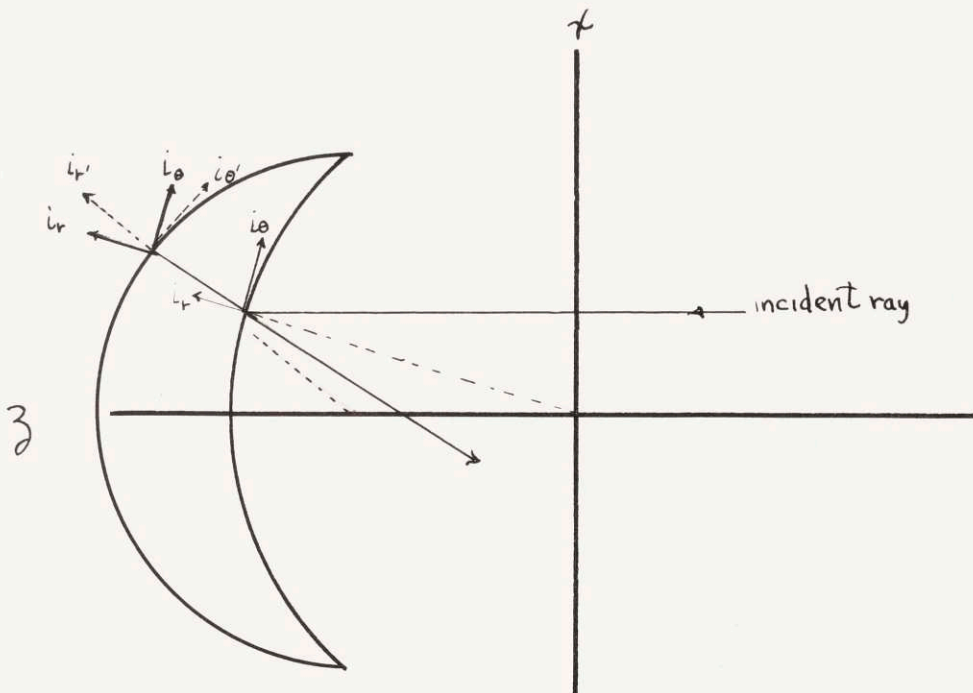
figure 11.

Solving for the unprimed components in terms of the primed system:

$$i_r = i_{r'}\cos(\theta' - \theta) - i_{\theta'}\sin(\theta' - \theta)$$

$$(2.46)$$

$$i_\theta = i_{r'}\sin(\theta' - \theta) + i_{\theta'}\cos(\theta' - \theta)$$

From the preceeding derivations it may be seen that equations
2.17, 2.30 and 2.29 provide sufficient information to form an expression
for the geometrical optics amplitude, phase and direction of the electric
field distribution over the reference sphere, based upon a desired
reflected field E_r. Quantities of interest, including the radii of curv-
ature of the wavefront, distance from the point of the reference sphere
under consideration to the corresponding point on the reflector, and the
relationship between angles are given by 2.43, 2.44, 2.33 and 2.40
respectively. Finally, transformation of the vector components given by
2.46 relates this field distribution to coordinates at the center of the
reference sphere. Thus the geometrical optics field is described over the
reference sphere as a function of the reflector surface under investiga-
tion and the particular origin of interest of the reference sphere.

In summary, we formulate an expression for the general case where a desired electric vector field is specified over the aperture. Choosing this field to have unity amplitude, we describe the field that would occur over the reference sphere:

Amplitude: $\qquad E_{\substack{reference \\ sphere}} = E_{reflector} \left| \dfrac{R_{1n} R_{2n}}{(R_{1n} + L_n)(R_{2n} + L_n)} \right|^{\frac{1}{2}} \qquad (2.17)$

Phase: $\qquad$ Phase$(E_{\substack{reference \\ sphere}}) \quad \propto \quad e^{jk_o R(\cos\theta - L_n)} \qquad\qquad (2.30)$

Direction: $\qquad E_{\substack{reference \\ sphere}} = \quad - E_r + 2(n \cdot E_r)n \qquad\qquad\qquad (2.29)$

Combining:

$$E_{\substack{reference \\ sphere}} = \left| \dfrac{R_{1n} R_{2n}}{(R_{1n} + L_n)(R_{2n} + L_n)} \right|^{\frac{1}{2}} e^{jk_o R(\cos - L_n)} \{-E_r + 2(n \cdot E_r)n\}$$

$$(2.47)$$

where:

$$R_{1n} = \frac{\cos\theta}{2} \tag{2.43}$$

$$R_{2n} = \frac{1}{2\cos\theta} \tag{2.44}$$

$$R'_n = \sqrt{1 + c^2 - 2c \cos\theta_m} \tag{2.31}$$

$$L_n = \sqrt{(\sin\theta - R'_n\sin\theta') + (R'_n \cos\theta' + c - \cos\theta)} \tag{2.33}$$

$$\cos\theta' = \frac{1}{R'_n} (\sin\theta\sin2\theta + c \cos^2 2\theta - c$$

$$+ \sqrt{\sin\theta\sin2\theta + c \cos^2 2\theta)^2 - \sin^2\theta + \cos^2 2\theta(R'^2_n - c^2)}) \tag{2.40}$$

$$i_r = i_{r'}\cos(\theta' - \theta) - i_{\theta'}\sin(\theta' - \theta)$$

$$\tag{2.46}$$

$$i_\theta = i_{r'}\sin(\theta' - \theta) + i_{\theta'}\cos(\theta' - \theta)$$

E = E_0 i_x e^{jk_o z}

propagation

H = -H_0 i_y e^{jk_o z}

aperture, side projection

figure 12

2.5   In this section, we apply the results of the general expression 2.47

to a particular case of interest. Specifying the field at the aperture

shown in figure 12 to be a uniform plane wave linearly polarized in the

x- direction we have:

$$E_{aperture} = i_x \, e^{jk_o z}$$

Expanding in spherical coordinates:

$$E_{aperture} = e^{jk_o R\cos\theta} \, (\, i_r \sin\theta \cos\phi + i_\theta \cos\theta \cos\phi - i_\phi \sin\phi) \qquad (2.48)$$

By applying equation 2.29, reversing the sense of tangential components,

we can determine the sense of direction of the field over the reference

sphere:

56

$$\text{direction}(\ E_{\substack{\text{reference} \\ \text{sphere}}}) \ = \ i_r \sin\theta\cos\phi - i_\theta\cos\theta\cos\phi + i_\phi\sin\phi \quad (2.49)$$

Applying equations 2.46 to 2.49 the direction of the field vector can be expressed in terms of the origin at that of the reference sphere:

$$i_r = i_{r'}\cos(\theta' - \theta) - i_{\theta'}\sin(\theta' - \theta)$$

$$(2.46)$$

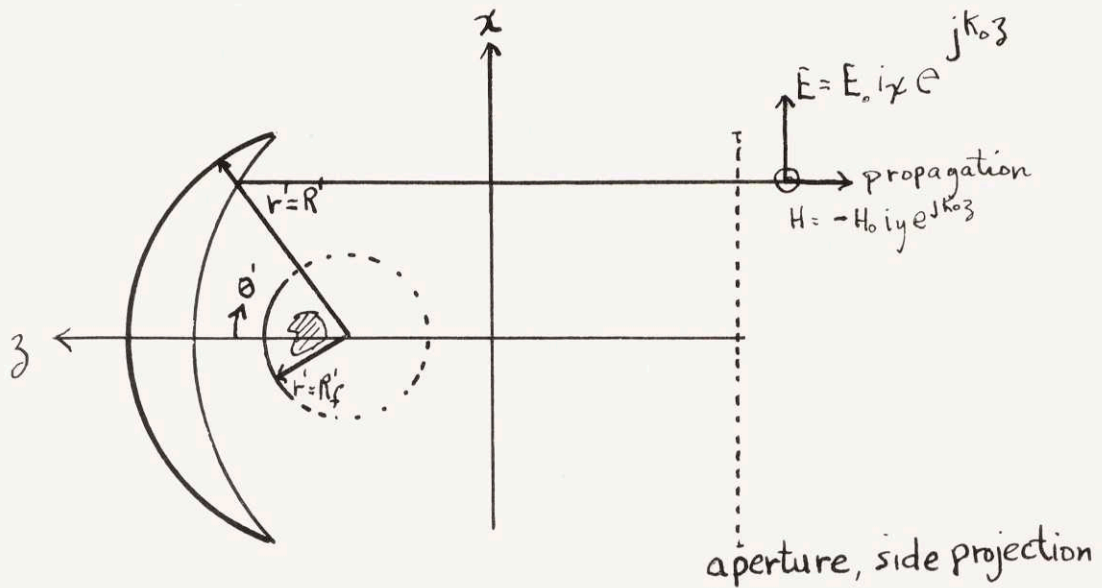$$i_\theta = i_{r'}\sin(\theta' - \theta) + i_{\theta'}\cos(\theta' - \theta)$$

Substituting:

$$\text{direction}(\ E_{\substack{\text{reference} \\ \text{sphere}}}) \ = \ i_{r'}\cos\phi\ (\ \sin\theta\cos(\theta' - \theta) - \cos\theta\sin(\theta' - \theta))$$

$$- i_{\theta'}\cos\phi(\ \sin\theta\sin(\theta' - \theta) + \cos\theta\cos(\theta' - \theta))$$

$$+ i_\phi\sin\phi \quad\quad\quad\quad\quad (2.50)$$

Collecting terms and applying trigonometric identities for the difference of angles we obtain:

$$\text{direction}\ (\ E_{\substack{\text{reference} \\ \text{sphere}}}) \ = \ i_{r'}\cos\phi\sin(2\theta - \theta') - i_{\theta'}\cos\phi\cos(2\theta - \theta')$$

$$+ i_\phi\sin\phi \quad\quad\quad\quad\quad (2.51)$$

Thus from previously developed relationships 2.17 and 2.30, expressions
for amplitude, phase, and direction of the electric field over the ref-
erence sphere can be combined to yield the vector field solely as a
function of the particular reflector under investigation and the choice
of origin of the reference sphere along the axis.

While simplification could be performed on the resluting expression,
the field over the reference sphere is, in itself, only a means to
eventually describe the fields over a smaller sphere surrounding some
source region, concentric with the reference sphere. Since the simplifica-
tion would not enhance this procedure, it will not be pursued. Rather,
the resulting expression

$$
E_{\substack{\text{reference}\\\text{sphere}}} = \left| \frac{R_{1n}R_{2n}}{(R_{1n} + L_n)(R_{2n} + L_n)} \right|^{\frac{1}{2}} \quad e^{jk_0 R(\cos\theta - L_n)} \quad X
$$

$$
(\ i_r \cdot \cos\phi\sin(2\theta - \theta') - i_\theta \cdot \cos\phi\cos(2\theta - \theta') + i_\phi \sin\phi\ )
$$

$$
(2.52)
$$

(where R_{1n}, R_{2n}, L_n and angle relationships are defined by 2.43,
2.44, 2.33, and 2.40 and are listed for convenience in section 2.4)

lends itself readily to tecniques of machine computation. As a result,
the following pages contain graphs representing the field components
in amplitude and phase for a particular choice of parameters. The results
are calculated for normalized amplitude and reflect no variation in the

azimuthal ϕ direction. Thus the components E_θ, and E_ϕ indicated in the graph must be multiplied by $\cos\phi$ and $\sin\phi$ respectively to represent the true nature of the field over the entire sphere. Similarly, the E_r, component must be multiplied by the variation $\cos\phi$. The computer program developed to calculate the field over the reference sphere is included in appendix II.

NORMALIZED AMPLITUDE
OF FIELD COMPONENTS
ON REFERENCE SPHERE $R' = .665R$, origin at $z = .52R$
FOR REFLECTOR RADIUS $R = 93\lambda$, $\Theta m = 37.4°$

$-E_\theta$

E_ϕ

Er

θ' degrees

FIGURE 13

60
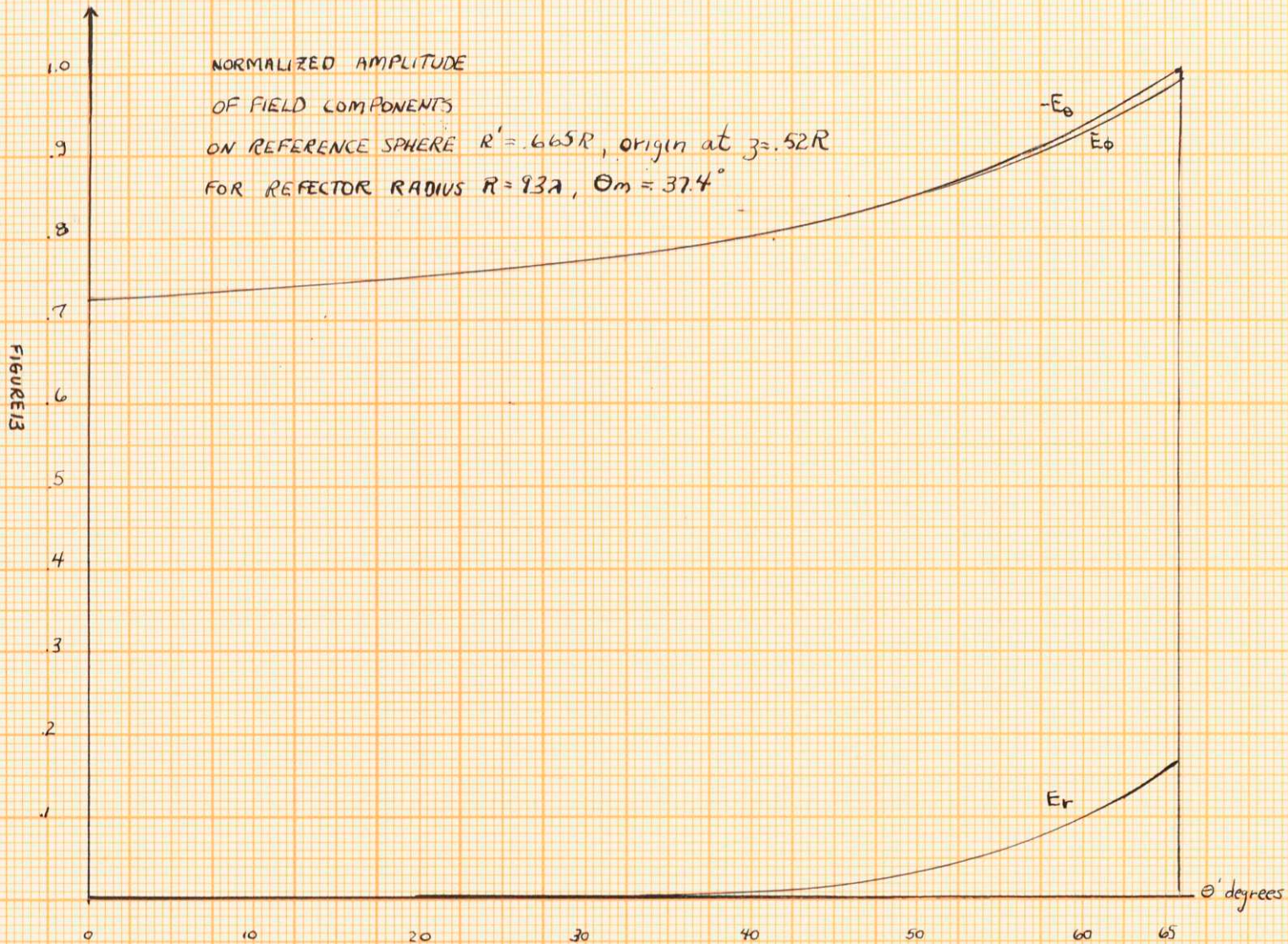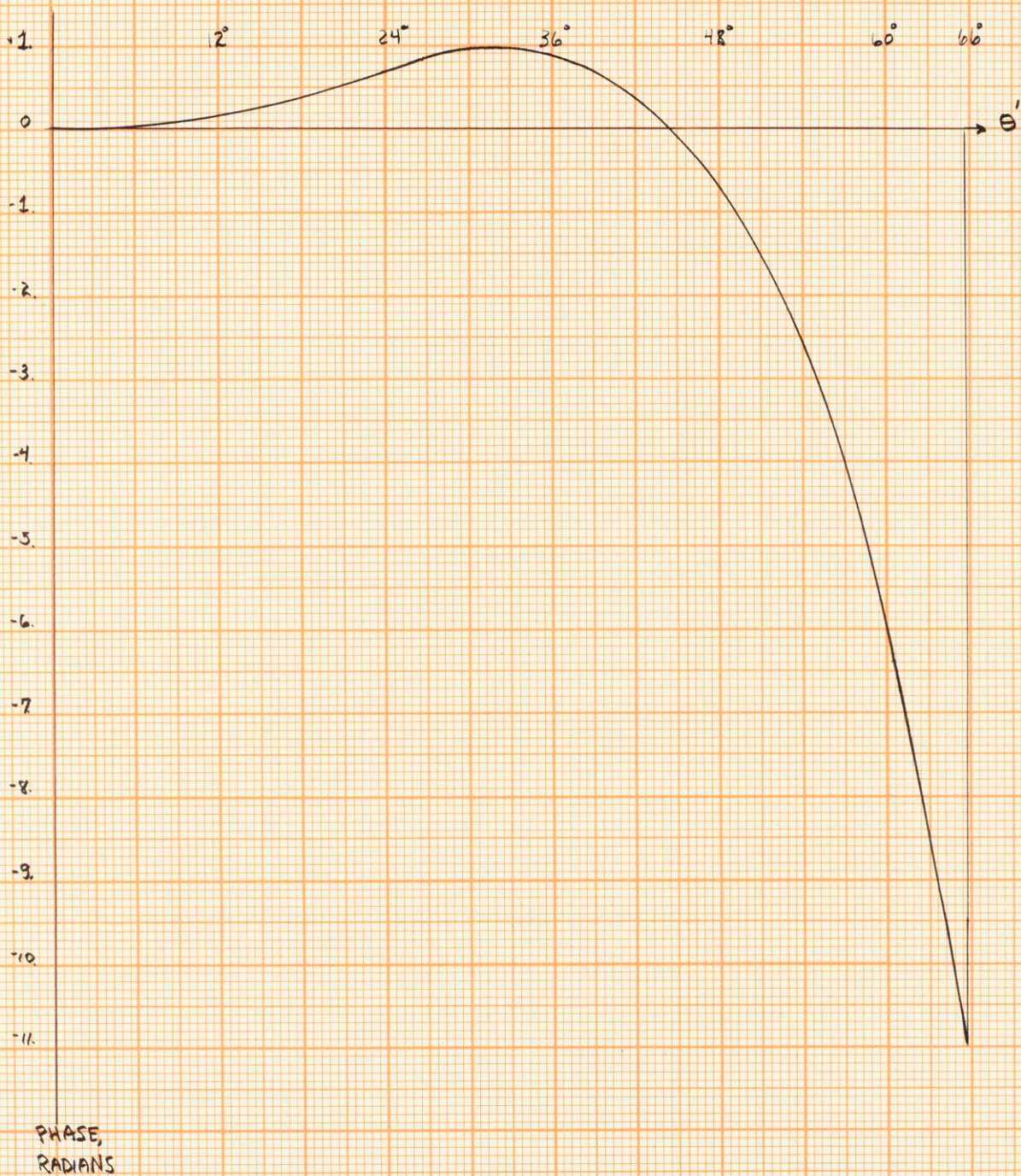
PHASE, IN RADIANS, VS. ANGLE θ', IN DEGREES
FOR REFLECTOR OF RADIUS R= 93λ, θ_m= 37.4°
CENTER OF REFERENCE SPHERE AT z = .52 R
REFERENCE SPHERE RADIUS R'= .665 R

figure 14

61

CHAPTER III

ELECTROMAGNETIC FIELD EQUATIONS, EXPANSION, AND SOLUTION

3.1   In the preceeding chapter expressions for the electric field over the
reference sphere were determined. In this chapter those fields will be
matched at the reference sphere to an expansion of spherical harmonics
following from solution to the vector wave equation in spherical coordi-
nates. These harmonics will be evaluated at a particular radius within
that of the reference sphere to yield the electric field over the surface
of that smaller sphere enclosing some source region. These fields will be
compared to the solution of Ricardi for the same region. Finally, these
results and the comparison of solutions will be interpreted.

It may be shown[34] that solution to the scalar Helmholtz equation

$$(\nabla^2 + k^2)\Psi = 0 \tag{3.1}$$

for spherical coordinates is given by separation of variables to be:

$$\Psi_{mn} = b_n(kr)\, P_n^m(\cos\theta)\, \begin{Bmatrix} \cos m\phi \\ \sin m\phi \end{Bmatrix} \tag{3.2}$$

where $b_n(kr)$ is the spherical Bessel function and $P_n^m(\cos\theta)$ is the
associated Legendre function of the first kind. The choice of $\cos m\phi$
or $\sin m\phi$ depends upon the variation of the fields at the boundary of
interest.

The fields under investigation in chapter 2 were shown to be vector
fields, and the solution to the vector Helmholtz equation must be
considered as:

$$(\nabla^2 + k^2)A = 0 \tag{3.3}$$

where A is a vector field, representing either the magnetic vector
potential or its dual, the electric vector potential. It has been
shown[35] that a general solution may be formulated by considering a set
of fields, both magnetic and electric, which are transverse to the
radial vector, i_r. In this case the solutions to 3.3 are found to be:

$$A = \psi^a \, r \, i_r$$

$$\tag{3.4}$$

$$F = \psi^f \, r \, i_r$$

where ψ is the solution to the scalar Helmholtz equation, with the super-
script indicating that is solution to the vector Helmholtz equation
for the magnetic potential A or the electric potential F.

The most general solution for fields in a source-free homogeneous region in terms of vector potentials is found to be[36] a linear combination of fields with the behavior of equations 3.4, where:

$$E = -\nabla \times F - j\omega\mu A + \frac{1}{j\omega\epsilon} \nabla (\nabla \cdot A)$$

$$(3.5)$$

$$H = \nabla \times A - j\tilde{\omega}\epsilon F + \frac{1}{j\omega\mu} \nabla (\nabla \cdot F)$$

Since the solutions for A and F involve the product of r and Ψ, it has been found convenient to adopt an alternative definition of the spherical Bessel function[37]:

$$\hat{H}_n^{(2)}(kr) = kr \, h_n^{(2)}(kr)$$

The superscript $\hat{H}_n^{(2)}$ indicates we have chosen the spherical Hankel function of the second kind, whose behavior indicates propagation outward from the origin, as applicable to this problem. Anticipating further, since the fields we wish to expand are of the form of equation 2.52, where the variation with ϕ is given by $\sin\phi$ and $\cos\phi$, we choose m = 1 . Thus:

$$A_r = \sum_n a_n \, \hat{H}_n^{(2)}(kr) \; P_n^1(\cos\theta) \begin{Bmatrix} \sin\phi \\ \cos\phi \end{Bmatrix}$$

$$(3.6)$$

$$F_r = \sum_n b_n \, \hat{H}_n^{(2)}(kr) \; P_n^1(\cos\theta) \begin{Bmatrix} \sin\phi \\ \cos\phi \end{Bmatrix}$$

64

Expanding equation 3.5 in component form we obtain:

$$E_r = \frac{1}{j\omega\varepsilon} \left(\frac{\partial^2}{\partial r^2} + k^2 \right) A_r$$

$$E_\theta = \frac{-1}{r\sin\theta} \frac{\partial F_r}{\partial \phi} + \frac{1}{j\omega\varepsilon r} \frac{\partial^2 A_r}{\partial r \partial \theta}$$

$$E_\phi = \frac{1}{r} \frac{\partial F_r}{\partial \theta} + \frac{1}{j\omega\varepsilon r\sin\theta} \frac{\partial^2 A_r}{\partial r \partial \phi}$$

$$H_r = \frac{1}{j\omega\mu} \left(\frac{\partial^2}{\partial r^2} + k^2 \right) F_r \qquad (3.7)$$

$$H_\theta = \frac{1}{r\sin\theta} \frac{\partial A_r}{\partial \phi} + \frac{1}{j\omega\mu r} \frac{\partial^2 F_r}{\partial r \partial \theta}$$

$$H_\phi = \frac{-1}{r} \frac{\partial A_r}{\partial \theta} + \frac{1}{j\omega\mu r\sin\theta} \frac{\partial^2 F_r}{\partial r \partial \phi}$$

Referring to the component E_θ in 3.7, we note that ϕ variation for A_r and $\frac{\partial F_r}{\partial \phi}$ is the same. Hence we choose the appropriate variation in equation 3.6. We note further that the function $P_n^1(\cos\theta)$ is identically zero for $n = 0$. The series need begin for $n = 1$, and may be written:

$$A_r = \sum_{n=1}^{\infty} a_n \hat{H}_n^{(2)}(kr) \; P_n^1(\cos\theta) \; \cos\phi$$

$$(3.8)$$

$$F_r = \sum_{n=1}^{\infty} b_n \hat{H}_n^{(2)}(kr) \; P_n^1(\cos\theta) \; \sin\phi$$

Substituting into the appropriate components of 3.7 the electric field can be formulated :

$$E_n = \frac{a_n \, n(n+1)}{j\omega\varepsilon r^2} \hat{H}_n^{(2)}(kr) \; P_n^1(\cos\theta) \; \cos\phi \; i_r$$

$$- \frac{1}{r\sin\theta} b_n \hat{H}_n^{(2)}(kr) \; P_n^1(\cos\theta) \; \cos\phi \; i_\theta$$

$$(3.9) \qquad + \frac{1}{j\omega\varepsilon r} a_n \cos\phi \frac{d\hat{H}_n^{(2)}(kr)}{dr} \frac{dP_n^1(\cos\theta)}{d\theta} \; i_\theta$$

$$+ \frac{1}{r} b_n \hat{H}_n^{(2)}(kr) \sin\phi \frac{dP_n^1(\cos\theta)}{d\theta} \; i_\phi$$

$$- \frac{1}{j\omega\varepsilon r \sin\theta} a_n \sin\phi \, P_n^1(\cos\theta) \frac{d\hat{H}_n^{(2)}(kr)}{dr} \; i_\phi$$

For convenience we define:

$$\frac{d \, \hat{H}_n^{(2)}(kr)}{dr} = k \, \frac{d \, \hat{H}_n^{(2)}(kr)}{d(kr)} = k \, \hat{H}_n^{(2)'}(kr)$$

and since we are concerned with the case of propagation in free space

$$k = k_o = \omega \sqrt{\epsilon_o \mu_o}$$

$$\zeta = \sqrt{\mu_o / \epsilon_o}$$

Substituting the relationships from above, multiplying through by $j/j = 1$, and including the summation we form equation 3.10 from 3.9 :

(3.10)

$$E = \frac{1}{r} \sum_{n=1}^{\infty} \left\{ \frac{+a_n \, n(n+1)}{j\omega\epsilon r} \, \hat{H}_n^{(2)}(kr) \, P_n^1(\cos\theta) \, \cos\phi \, i_r \right.$$

$$+ j\zeta a_n \, \hat{H}_n^{(2)'}(kr) \left[-\cos\phi \, \frac{d \, P_n^1(\cos\theta)}{d\theta} \, i_\theta + \frac{\sin\phi}{\sin\theta} \, P_n^1(\cos\theta) \, i_\phi \right]$$

$$+ \, b_n \, \hat{H}_n^{(2)}(kr) \left[\frac{-\cos\phi}{\sin\theta} \, P_n^1(\cos\theta) \, i_\theta + \sin\phi \, \frac{d \, P_n^1(\cos\theta)}{d\theta} \, i_\phi \right] \left. \right\}$$

67

Introducing tangential spherical harmonics as defined by Morse and
Feshback[38]:

$$B_{mn}^{e} = \frac{1}{\sqrt{n(n+1)}} \left[\cos m\phi \frac{dP_n^m(\cos\theta)}{d\theta} i_\theta - \frac{m\sin m\phi P_n^m(\cos\theta)}{\sin\theta} i_\phi \right]$$

(3.11)

$$C_{mn}^{o} = \frac{1}{\sqrt{n(n+1)}} \left[\frac{m\cos m\phi}{\sin\theta} P_n^m(\cos\theta) i_\theta - \sin m\phi \frac{dP_n^m(\cos\theta)}{d\theta} i_\phi \right]$$

Substituting 3.11 into 3.10 we can form an expression for the tangential
fields. By exploiting certain orthogonality properties of the tangential
harmonics, we can derive the constants a_n and b_n in 3.10 from the fields
specified at the boundary of interest. In our problem, it will be the
tangential fields on the reference sphere that will be specified. Note
that from equation 3.10 the two constants a_n and b_n are sufficient to
describe the field vector. It must also be noted that development of all
expressions in this chapter has proceeded for the case where the origin
of the sphere for which boundary conditions were given coincided with
the origin of the coordinate system for the spherical harmonics. It now
becomes necessary to stipulate that the harmonics must be expanded about
an origin at the center of the reference sphere. To adapt these expression
we need only to substitute θ' for θ, recognizing that the angle is de-
fined as in chapter 2, and for the radius variable r we substitute r',
indicating that it is measured from the prime coordinate origin.

From the preceeding we can write for the tangential field components:

$$E_{tang} = -\frac{1}{r} \sum_{n=1}^{\infty} \sqrt{n(n+1)} \left[b_n \hat{H}_n^{(2)}(kr)\, C_{1n}^{o} + j\zeta a_n \hat{H}_n^{(2)'}(kr)\, B_{1n}^{e} \right]$$

$$(3.12)$$

Coefficients are evaluated by forming the vector dot product $C_{1q} \cdot E_{tang}$, multiplying each side of 3.12 by $\sin\theta d\theta d\phi$, integrating over the interval $0-\pi$ and $0-2\pi$ on ϕ and θ respectively, evaluating the fields at the reference sphere, radius R'. The following properties are listed below:[39]

$$\int \int \begin{matrix} B_{1q}^{e} \cdot B_{1n}^{e} \\ C_{1q}^{o} \cdot C_{1n}^{o} \end{matrix} \sin\theta d\theta d\phi = \begin{matrix} \dfrac{2\pi n(n+1)}{2n+1} & n=q \\ \\ 0 & n \neq q \end{matrix}$$

$$\int \int C_{1n}^{o} \cdot B_{1q}^{e} \sin\theta d\theta d\phi = 0 \quad \text{for all } n,q$$

Applying these properties to equation 3.12 we have:

$$a_n = \frac{j(2n+1) \ R' \ \iint E_{rt} \cdot B_{1n}^e \ \sin\theta' d\theta' d\phi}{\zeta 2\pi H_n(kR') \ (n(n+1))^{3/2}}$$

$$(3.13)$$

$$b_n = \frac{-(2n+1) \ R' \ \iint E_{rt} \cdot C_{1n}^\theta \ \sin\theta' d\theta' d\phi}{2\pi H_n(kR') \ (n(n+1))^{3/2}}$$

where E_{rt} is the vector representation of the tangential components of the electric field over the reference sphere at radius R'. To perform the integration indicated in equations 3.13 we proceed by expanding the field E_{rt} in a fourier series. We choose a series appropriate for the fields over the reference sphere, in this case a series with even symmetry about $\theta' = 0$, and where the ϕ dependence matches that of the fields at the boundary, as suggested by equation 2.52. Proceeding:

$$E_{rt}(R',\theta',\phi) = \sum_{m=0}^{\infty} (c_m \cos\phi \ i_{\theta'} + d_m \sin\phi \ i_\phi) \cos m\theta' \quad (3.14)$$

The fourier coefficients are obtained in the normal fashion, and are covered in appendix 2.

Consistent with the notation of Ricardi we define coupling coefficients

$$I_{mn}^c = \int_0^\pi \cos m\theta' \ P_n^1(\cos\theta') \ d\theta'$$

$$(3.15)$$

$$I_{mn}^d = \int_0^\pi \cos m\theta' \ \sin\theta' \ \frac{d \ P_n^1(\cos\theta')}{d\theta'} \ d\theta'$$

70

Substitution of 3.15 into 3.13, using the definition of fourier co-
efficients from 3.14 we obtain:

$$a_n = \frac{j A_n R'}{H_n'(kR')} \sum_{m=0}^{\infty} (c_m I_{mn}^d - d_m I_{mn}^c)$$

$$(3.16)$$

$$b_n = \frac{- A_n R'}{H_n(kR')} \sum_{m=0}^{\infty} (c_m I_{mn}^c - d_m I_{mn}^d)$$

where

$$A_n = \frac{2n + 1}{2(n(n+1))^2}$$

Therefore to fully express the electric field in the spherical harmonic
expansion we need only to evaluate the fourier coefficients in 3.14 and
the coupling coefficients given by 3.15. These coefficients, when sub-
stituted into the series 3.16 yield coefficients of the spherical
harmonic expansion.

These constants are normally evaluated by a recursion technique[40]
rather than solving for each term by evaluation of the integrals. This
recursion technique is particularly easy to realize with machine computa-
tion, and is inherent in Ricardi's method of evaluation. Thus coefficients
will be computed rather than analytically determined.

In summary the relationships that express the electric field as a spherical expansion of a specified field on a given reference sphere such as shown in figure 12 are listed:

$$E(r',\theta',\phi) = \frac{-1}{r'} \sum_{n=1}^{\infty} \left\{ \frac{-a_n \, n(n+1)}{j\omega\epsilon r'} \overset{\wedge(2)}{H}_n(kr') \; P_n^1(\cos\theta') \; i_{r'} \right.$$

(3.17)

$$\left. + \sqrt{n(n+1)} \left[b_n \overset{\wedge(2)}{H}_n(kr') \; C_{1n}^0 \; + \; j\zeta \, a_n \overset{\wedge(2)'}{H}_n(kr') \; B_{1n}^e \right] \right\}$$

where C_{1n}^0 and B_{1n}^e are given by equation 3.11 with m=1 :

$$\frac{1}{\sqrt{n(n+1)}} \left[\frac{\cos\phi}{\sin\theta'} P_n^1(\cos\theta') \; i_{\theta'} \; - \; \sin\phi \, \frac{dP_n^1(\cos\theta')}{d\theta'} \; i_\phi \right]$$

$$\frac{1}{\sqrt{n(n+1)}} \left[\cos\phi \, \frac{dP_n^1(\cos\theta')}{d\theta'} \; i_{\theta'} \; - \; \frac{\sin\phi}{\sin\theta'} P_n^1(\cos\theta') \; i_\phi \right]$$

and a_n and b_n given by equations 3.16:

$$a_n = \frac{j \, A_n \, R'}{\zeta \overset{\wedge(2)'}{H}_n(kr')} \sum_{m=0}^{\infty} (c_m \, I_{mn}^d - d_m \, I_{mn}^c)$$

$$b_n = \frac{- A_n R'}{\hat{H}_n^{(2)}(kr')} \quad \sum_{m=0}^{\infty} (c_m I_{mn}^c - d_m I_{mn}^d)$$

$$A_n = \frac{2n + 1}{2(n(n+1))^2}$$

and the coupling coefficients I_{mn}^c, I_{mn}^d given by 3.15:

$$I_{mn}^c = \int_0^{\pi} \cos m\theta' \ P_n^1(\cos\theta') \ d\theta'$$

$$I_{mn}^d = \int_0^{\pi} \cos m\theta' \sin\theta' \ \frac{d P_n^1(\cos\theta')}{d\theta'} \ d\theta'$$

The fourier expansion coefficents c_m and d_m are defined in equation 3.14:

$$E_{rt} = E_{rt}(R',\theta',\phi) = \sum_{m=0}^{\infty} (c_m \cos\phi \ i_{\theta'} + d_m \sin\phi \ i_{\phi}) \cos m\theta'$$

73

E_{rt} is the vector representation of the electric field tangential to the reference sphere, as determined from 2.52.

While the series representation gives an accurate solution for the sum of all terms, it is recognized that this is impractical to realize. An important section of Ricardi's thesis dealt with justification of an appropriate truncation of the series solution[41]. That analysis deals with subjects beyond the scope of the present work, although it will be noted that the series truncation stems from a desire to avoid generation of highly reactive waves that do not, in practice, yield that much accuracy to the end result. On the basis of a rigorous analysis regaeding genera- tion of these highly reactive waves[42], it will suffice here to state that satisfactory results are obtained with the spherical expansion when the number of terms of the series is on the order of $N = kR_1'$, where R_1' is the particular radius at which evaluation is desired.

Therefore, equation 3.17, evaluated at $r' = R_f'$, where R_f' is the radius enclosing the transmitting feed which will produce the desired field

$$E_{\substack{\text{reference} \\ \text{sphere}}}$$

specified by equation 2.52, which will in turn produce after reflection a desired field distribution at the aperture, yields

$$E_{\substack{\text{feed} \\ \text{sphere}}} = E_f(R_f', \ \theta', \ \phi).$$

The equations for magnetic fields over the feed sphere can be obtained from Maxwell's equations. In particular:

$$H_{\substack{feed \\ sphere}} = - \frac{1}{j\omega\mu} \; \nabla \times E_{\substack{feed \\ sphere}}$$

In this analysis we have concentrated on solution of the electric fields at various boundaries. To produce the desired fields at the aperture it is not necessary to separately excite both $E_{\substack{feed \\ sphere}}$ and $H_{\substack{feed \\ sphere}}$, since through Maxwell's equations, the existance of one field specifies the other.

3.2 To illustrate the principles outlined in preceeding
sections and to show that these principles provide an
economical and efficient method of mathematical expansion
of fields from the geometrical optics reference sphere to
an interior feed sphere, a particular case was chosen for
evaluation.

The parameters of interest were chosen for $c = .52$,
representing a displacement of the origin of the feed and
reference spheres to $z = .52R$ for a reflector of radius
$R = 93\lambda$ and subtended angle of 37.4 degrees. The field
distribution of magnitude and phase were presented in
graphical form in section 2.5 for this choice of parameters.
Figure 3 of section 2.1 illustrates the geometry of the
eccentric coordinate system.

It must be noted that the choice of eccentric origin
chosen for this case of investigation was rather arbitrary,
as was the choice of inner sphere radius. This choice was
guided, however, from principles of geometrical optics. The
rays incident upon the extreme edge of the reflector surface
are reflected into the focal region, forming the caustic
surface. The points at which the edge rays are tangent to
the caustic surface define the marginal surface focus, that
plane surface generated by the rotation of B-B' of figure
15 about the axis of revolution of the reflector.

incident ray

x

θ_m

y

CAUSTIC SURFACE

A

A'

B

B'
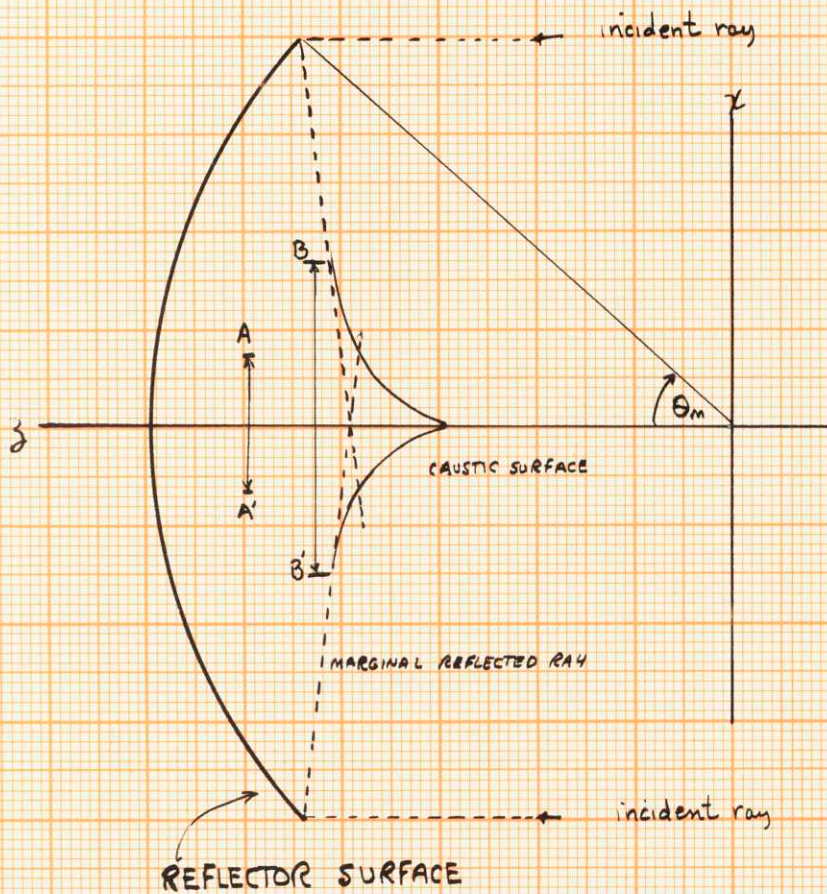
MARGINAL REFLECTED RAY

incident ray

REFLECTOR SURFACE

figure 15

Note that all reflected rays must pass through this surface. The smallest such surface through which all reflected rays must pass is defined by the circle of least confusion, generated by rotation of A-A' of figure 15 about the axis of symmetry.

While geometrical optics wrongly predicts infinite fields in the vicinity of caustics, the fact remains that converging rays indicate an area of energy concentration. Hence, an intuitive choice of probable location for a minimum-sized feed would be that aperture which most closely coincides with the circle of least confusion associated with a particular reflector. It is a simple matter to show from the geometry that a choice of origin between $z = .5R$ and $.6R$ requires a feed sphere on the order of 5-10 λ for a reflector of 93 λ with subtended angle 37.4 $^\circ$, as considered in this study, to meet these specifications. Hence, a representative distribution of fields over such a feed sphere that would be required by the tangential boundary conditions to yield a uniform plane wave over the reflector aperture is given by figures 16. Amplitude and phase of three components of electric field over the surface of a feed sphere of radius 8.4 λ with origin at $z = .52R$ for a reflector of radius $R = 93$ λ are presented in figures 16 A-F. This solution is a graphical result, obtained from evaluation of the series solution given by equation 3.16 and 3.17 of section 3.1.
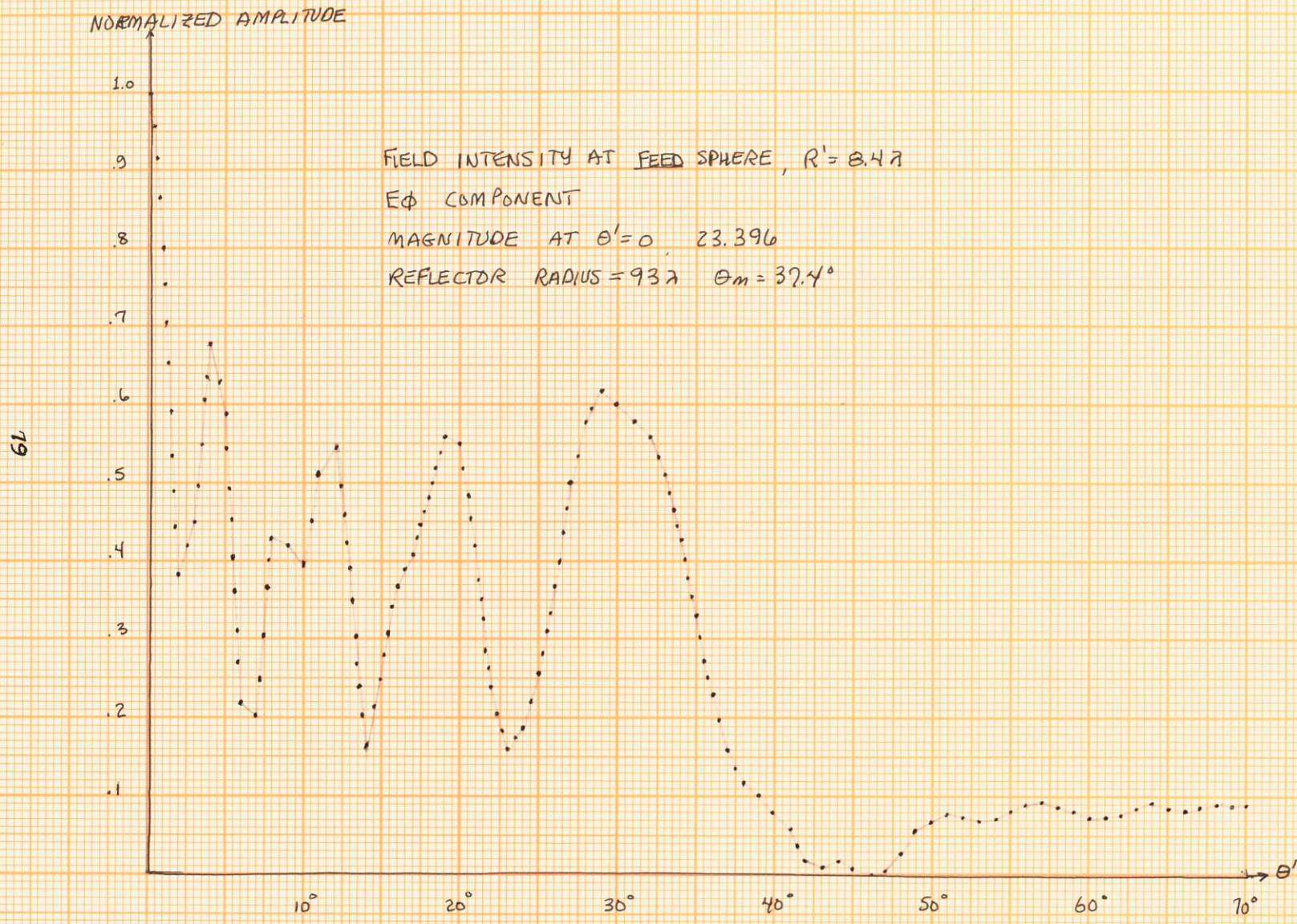
FIGURE 16-A

NORMALIZED AMPLITUDE
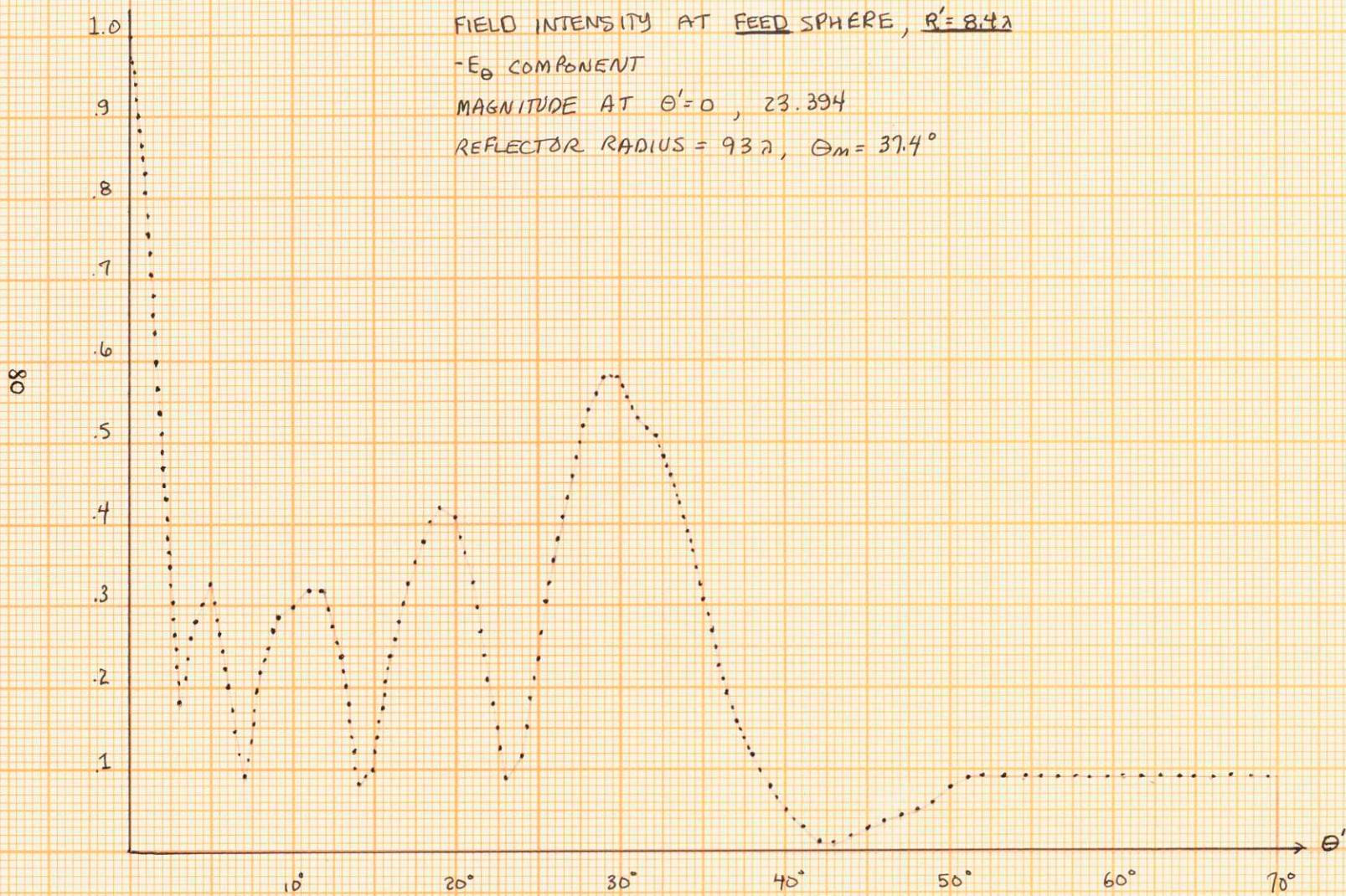
FIELD INTENSITY AT FEED SPHERE, $R' = 8.4\lambda$

-E_θ COMPONENT

MAGNITUDE AT $\theta' = 0$, 23.394

REFLECTOR RADIUS = 93λ, $\theta_m = 37.4°$

FIGURE 16-B

80

NORMALIZED AMPLITUDE

FIELD INTENSITY AT FEED SPHERE, $R' = 8.4\lambda$

E_r COMPONENT

MAGNITUDE AT $\theta' = 0$, 18.256

REFLECTOR RADIUS $= 93\lambda$, $\theta m = 37.4°$

FIG.16-C

PHASE OF FIELD DISTRIBUTION
OF Eϕ COMPONENT OVER
FEED SPHERE R'=8.4λ
CENTER AT Z̄=.52R
REFLECTOR RADIUS R=93λ

PHASE, RADIANS   FIGURE 16-D

82

PHASE OF FIELD DISTRIBUTION
OF $-E_\theta$ COMPONENT OVER
FEED SPHERE $R'= 8.4\lambda$
CENTER AT $z = .52R$
REFLECTOR RADIUS $R = 93\lambda$

PHASE, RADIANS

FIGURE 16-E

83

FIGURE 16-F

PHASE OF E_r
OVER FEED SPHERE
$R' = 8.4\lambda$, CENTER AT
$Z = .52R$, $R = 93\lambda$
$\Theta m = 37.4$

PHASE, RADIANS
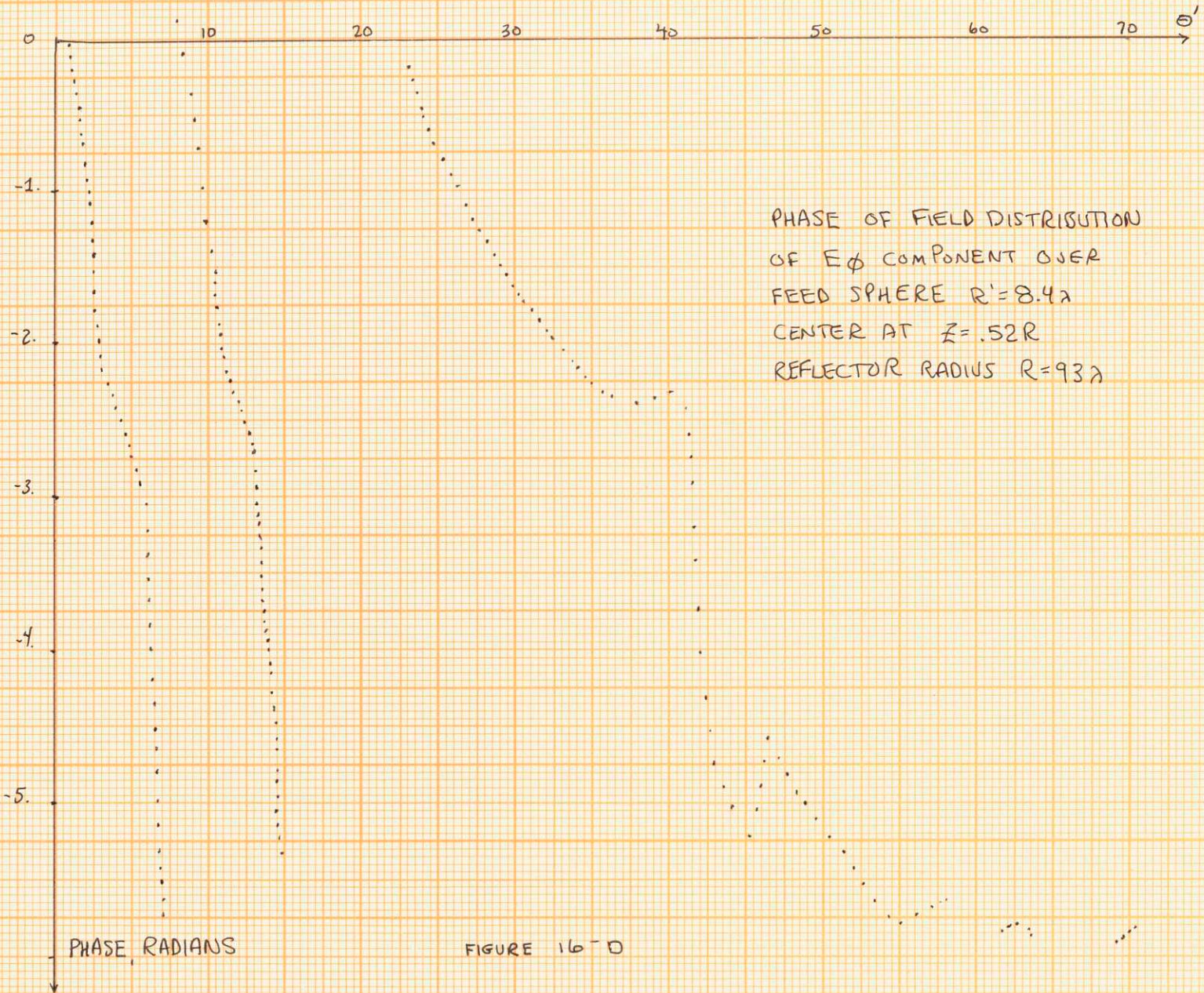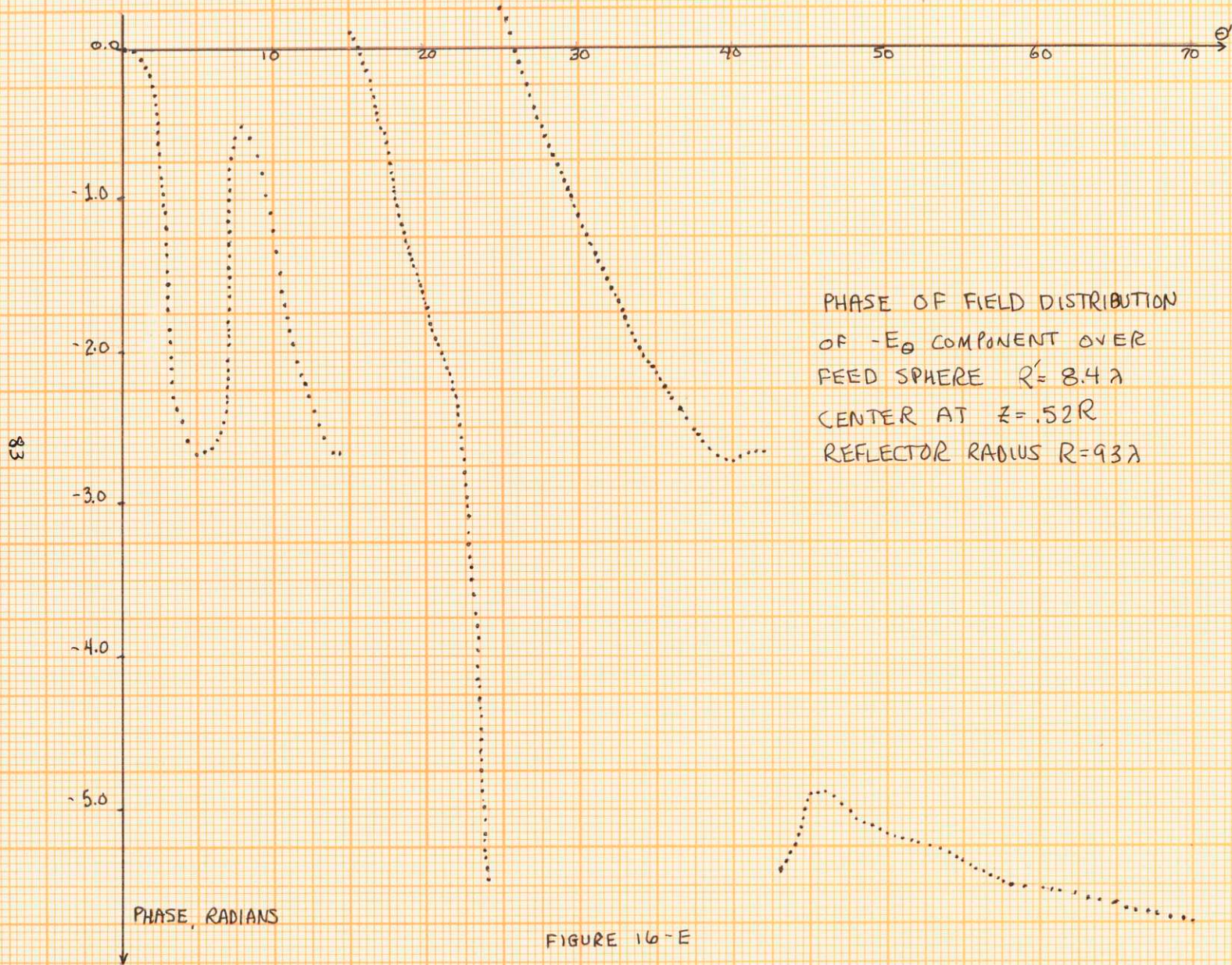
84

3.3 For the choice of parameters indicated in section 3.2
the magnitude and phase of the field distribution over the
reference sphere, as given by equation 2.52, were presented
in graphical form as figures 13 and 14 of section 2.5. The
nearly identical distribution of tangential components and
the near-vanishing radial component of the field are due
to the relationship between angular variables θ and θ',
where to first order ;

$$2\theta = \theta'$$

Only the tangential field components are used in the
boundary condition to generate the fourier coefficients,
as noted in appendix II. The tangential fields were expanded
in the following manner from equation 2.52:

$$E_{tan} = (\ E_\theta \cos\phi i_\theta, + E_\phi \sin\phi i_\phi\ )e^{j\psi}$$

$$E_{tan} = E_\theta \cos\phi (\cos\psi + j\sin\psi)\ i_\theta + E_\phi \sin\phi (\cos\psi + j\sin\psi) i_\phi$$

The real and imaginary parts, less the cosϕ, sinϕ dependence were then plotted graphically and are presented as figures 17 and 18 . Due to the similarity of magnitudes resulting from the nearly-identical nature of tangential components indicated by figures 13 and 14 of section 2.5, only two rather than four plots are presented here. The calculations, however, retain the existence of four separate components, two real and two imaginary, of tangential fields. These components were then expanded into a fourier series of the form:

$$E_{tan} = \sum_{m=0}^{M} (c_m \cos\phi \ i_{\theta'} + d_m \sin\phi \ i_{\phi})\cos m\theta$$

where c_m, d_m are now complex fourier coefficients determined as noted in appendix II, and M is the limiting value of the highest harmonic desired, given, as noted previously, by

$$M \simeq kr$$

with r the radius of observation.

DISTRIBUTION OF REAL PART OF NORMALIZED
TANGENTIAL FIELD COMPONENTS OVER
REFERENCE SPHERE FOLLOWING
EXPANSION OF THE FORM:

$$E_t = (E_\theta i_\theta + E_\phi i_\phi)e^{j\psi} = E_\theta(\cos\psi + j\sin\psi)_{i_\theta} + E_\phi(\cos\psi + j\sin\psi)_{i_\phi}$$

REFLECTOR RADIUS = 93λ, θ_m = 37.4°
ECCENTRIC ORIGIN AT Z = .52R
REFERENCE SPHERE RADIUS R' = .665R

figure 17

$-E_\theta \sin \psi$
$E_\phi \sin \psi$

1.0

.8

.6

.4

.2

0   10   20   30   40   50   60   66 θ'

88

-.2
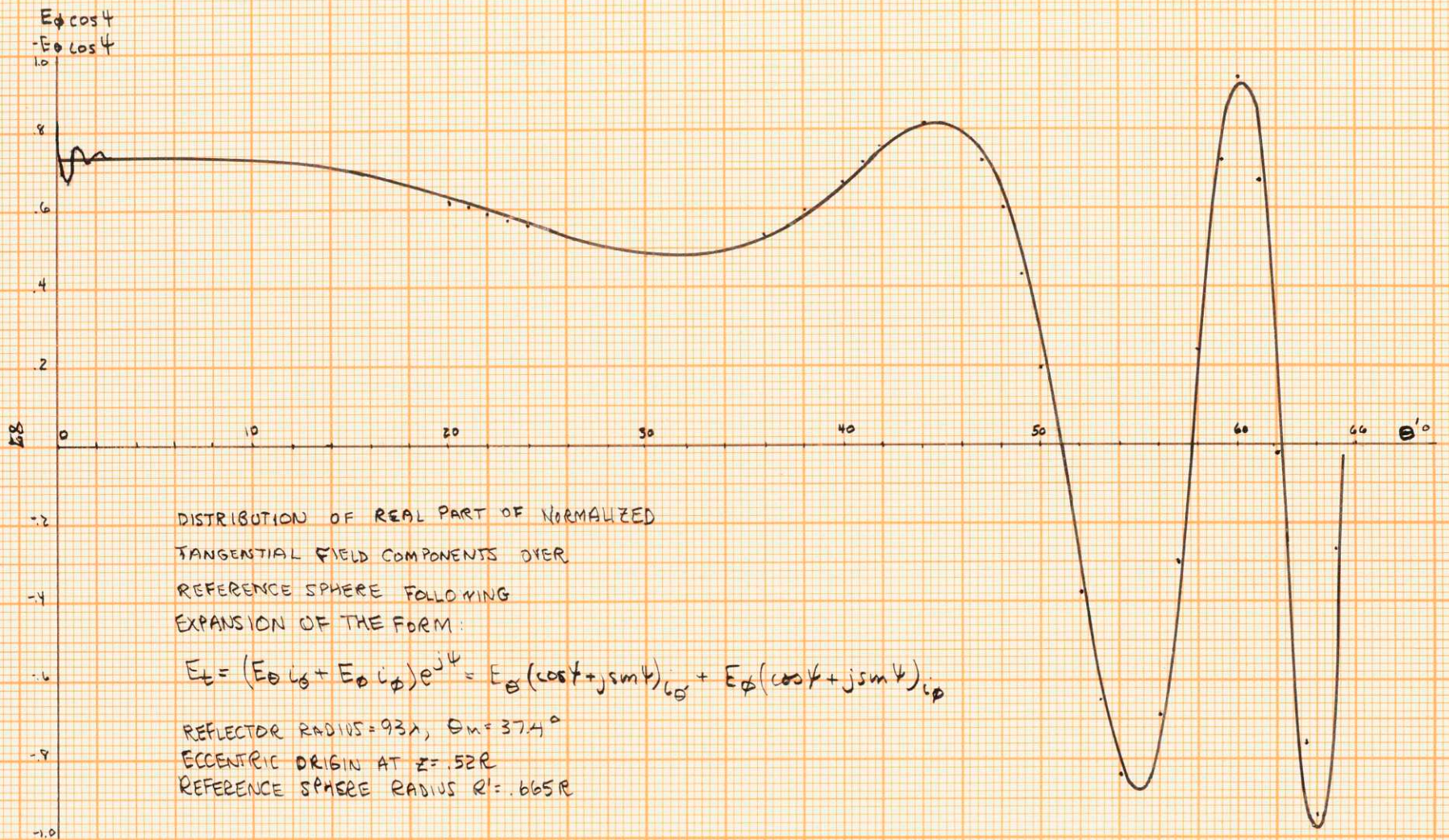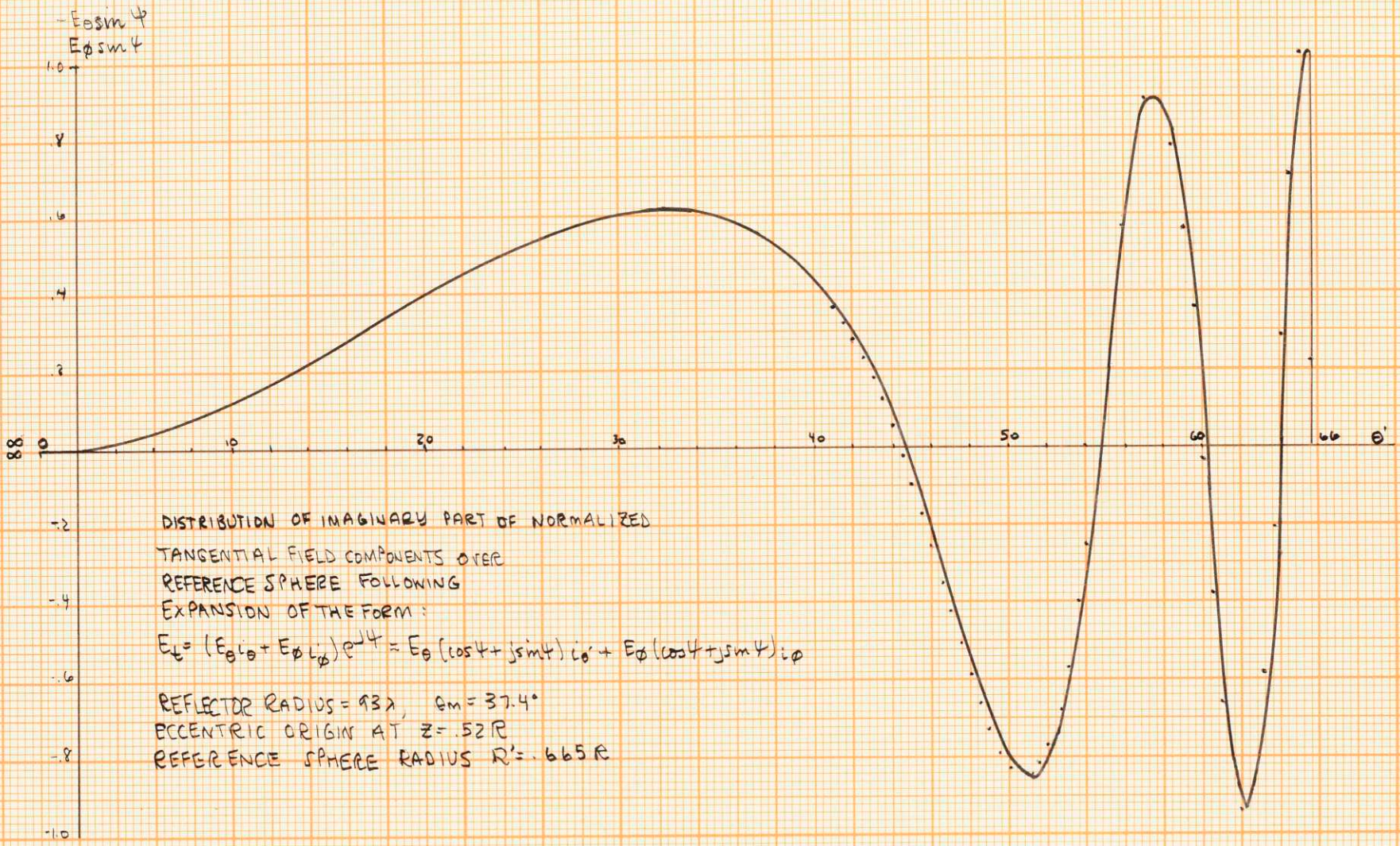
DISTRIBUTION OF IMAGINARY PART OF NORMALIZED

-.4

TANGENTIAL FIELD COMPONENTS OVER
REFERENCE SPHERE FOLLOWING
EXPANSION OF THE FORM:

$E_t = (E_\theta \, i_\theta + E_\phi \, i_\phi) e^{j\psi} = E_\theta (\cos \psi + j \sin \psi) i_\theta' + E_\phi (\cos \psi + j \sin \psi) i_\phi$

-.6

REFLECTOR RADIUS = 93λ, $\theta_m = 37.4°$
ECCENTRIC ORIGIN AT $z = .52R$
REFERENCE SPHERE RADIUS $R' = .665R$

-.8

-1.0

figure 18

To check on the accuracy of the fourier expansion technique, the series was summed using coefficients determined by the geometrical optics field over the reference sphere. The results are indicated in figures 17 and 18 as small departures from the heavy dark line, which represents the values used to generate the fourier coefficients.

These fourier coefficients were then used with the series solution, given by equations 3.16 and 3.17, to evaluate the fields at the reference sphere. The trends and accuracy of this series solution, when compared to the geometrical optics field initially calculated and subsequently used to generate the necessary coefficients, appears to be reasonable when viewed in figures 19. It is to be recalled that the series was truncated at a value of terms much less than infinite in order to avoid generation of highly reactive fields. The presentation of figures 19 involved 390 terms. As the series' accuracy improves with the number of terms, better agreement between the geometrical optics and resulting synthesized fields would theoretically be forthcoming with continued summation. It is to be noticed that the agreement of phase appears quite good for the tangential fields and satisfactory for the radial component. Similar agreement occurs in amplitude. The basic boundary condition that was involved required matching of the tangential fields so as to force the field to zero at the reflector surface. Hence, the radial component is also determined from this boundary condition, and should contain some variation for less than an infinite number of terms. The phase of the radial component is similarly determined from the real and imaginary parts of the component, and for the radial component

of near-zero magnitude, the error involved in the difference of small numbers begins to override the solution. Hence, for values of radial component near zero, rapid phase variations were encountered. These were not plotted as not being significant they added no contribution to the work.
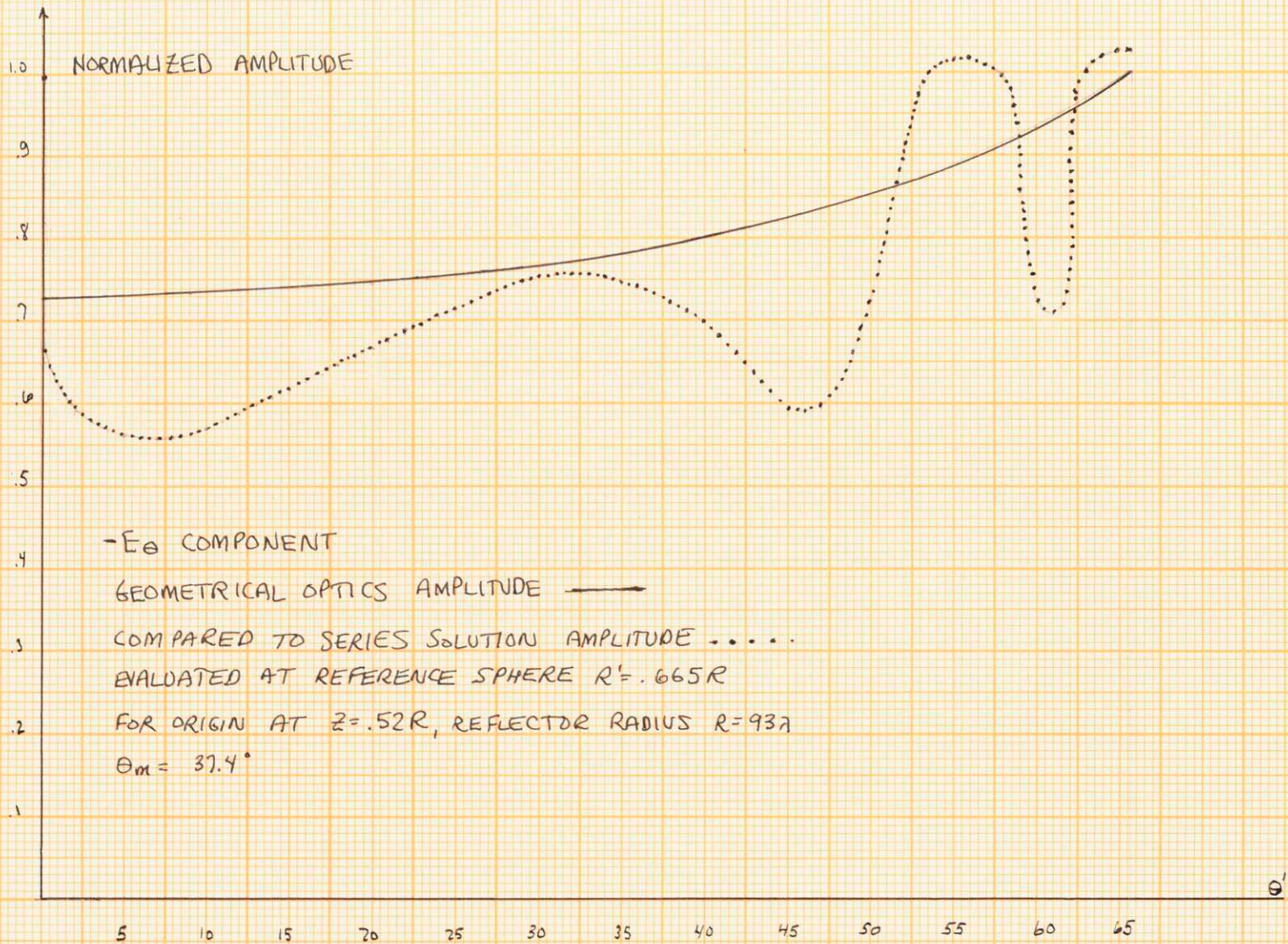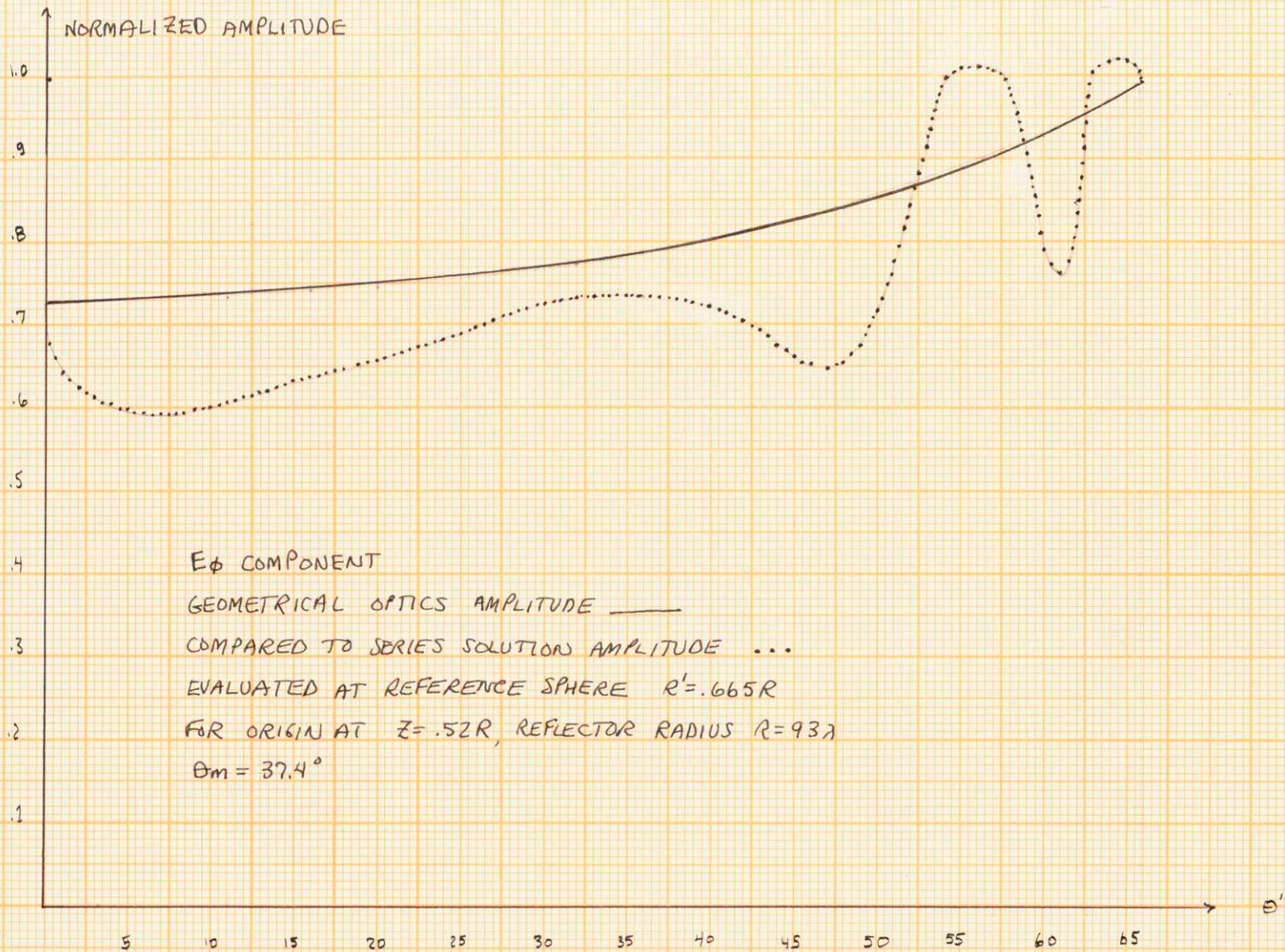
NORMALIZED AMPLITUDE

1.0
.9
.8
.7
.6
.5
.4   −E$_\theta$ COMPONENT
.3   GEOMETRICAL OPTICS AMPLITUDE ——
        COMPARED TO SERIES SOLUTION AMPLITUDE .....
        EVALUATED AT REFERENCE SPHERE R′=.665R
.2   FOR ORIGIN AT Z=.52R, REFLECTOR RADIUS R=93λ
        θ_m = 37.4°
.1

5   10   15   20   25   30   35   40   45   50   55   60   65   θ′

91

FIGURE 19-A

NORMALIZED AMPLITUDE

92

Eφ COMPONENT
GEOMETRICAL OPTICS AMPLITUDE _____
COMPARED TO SERIES SOLUTION AMPLITUDE ...
EVALUATED AT REFERENCE SPHERE   R'=.665R
FOR ORIGIN AT   Z=.52R, REFLECTOR RADIUS R=93λ
θm = 37.4°

FIGURE 19-B

NORMALIZED AMPLITUDE

93

E_r COMPONENT
GEOMETRICAL OPTICS AMPLITUDE ___
COMPARED TO SERIES SOLUTION AMPLITUDE ...
EVALUATED AT REFERENCE SPHERE $R'= .665R$
FOR ORIGIN AT $Z= .52R$, REFLECTOR RADIUS $R=93\lambda$
$\theta m = 37.4$

FIGURE 13-C

−E_θ COMPONENT

GEOMETRICAL OPTICS PHASE _____

COMPARED TO SERIES SOLUTION PHASE ••••

EVALUATED AT REFERENCE SPHERE $R' = .665R$

FOR ORIGIN AT $Z = .52R$, REFLECTOR RADIUS $R = 93\lambda$

$\theta_m = 37.4°$,

FIGURE 19-D

94

Eφ COMPONENT
GEOMETRICAL OPTICS PHASE ____
COMPARED TO SERIES SOLUTION PHASE . . . .
EVALUATED AT REFERENCE SPHERE $R' = .665R$
FOR ORIGIN AT $Z = .52R$, REFLECTOR RADIUS $R = 93\lambda$
$\theta_m = 37.4°$

PHASE, RADIANS   FIGURE 19-E

95

E_r COMPONENT

GEOMETRICAL OPTICS PHASE _____

COMPARED TO SERIES SOLUTION PHASE . . . .

EVALUATED AT REFERENCE SPHERE $R'=.665R$

FOR ORIGIN AT $Z=.52R$, REFLECTOR RADIUS $R=93\lambda$

$\theta_m = 32.4°$

FIGURE 19-F

PHASE,
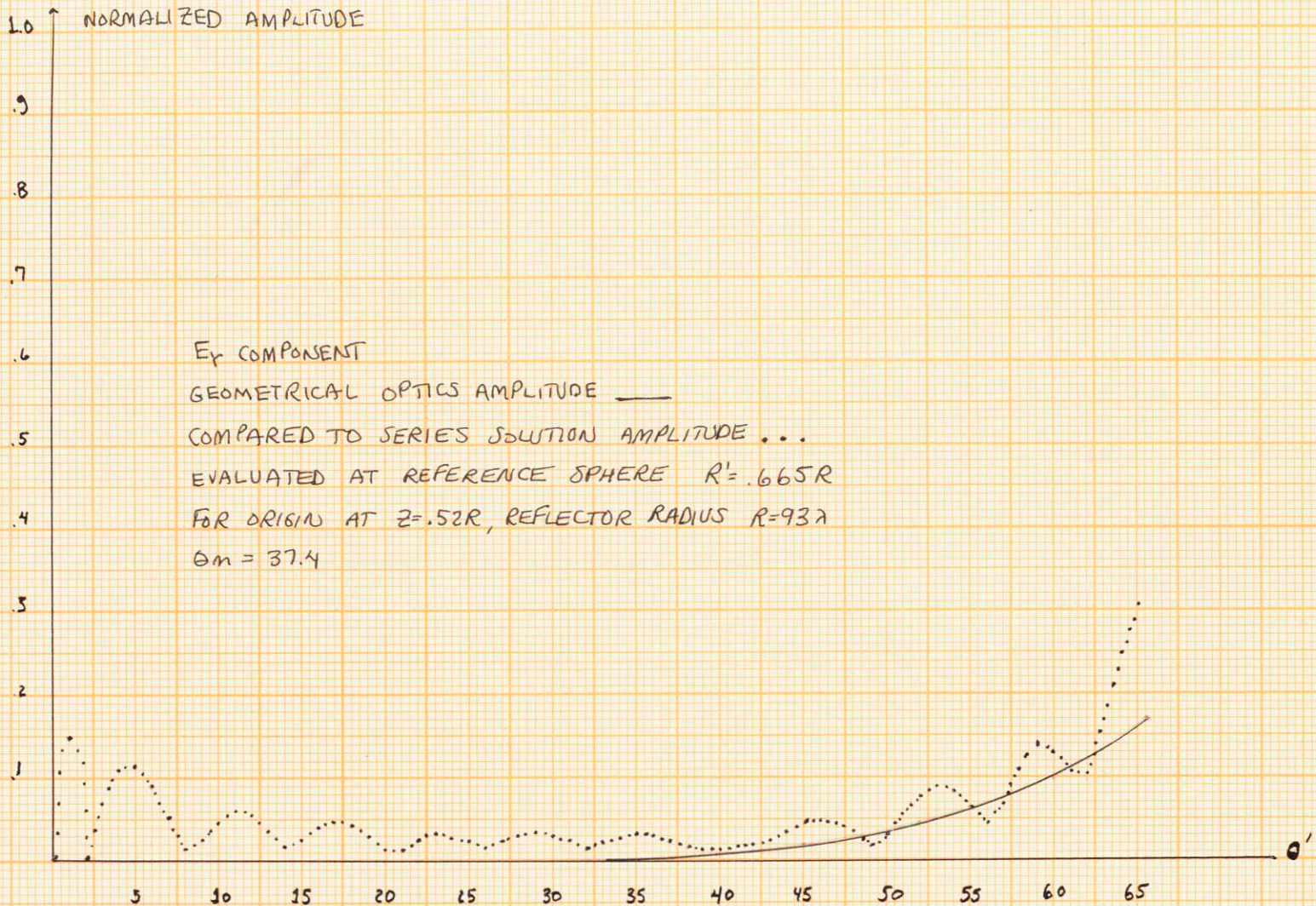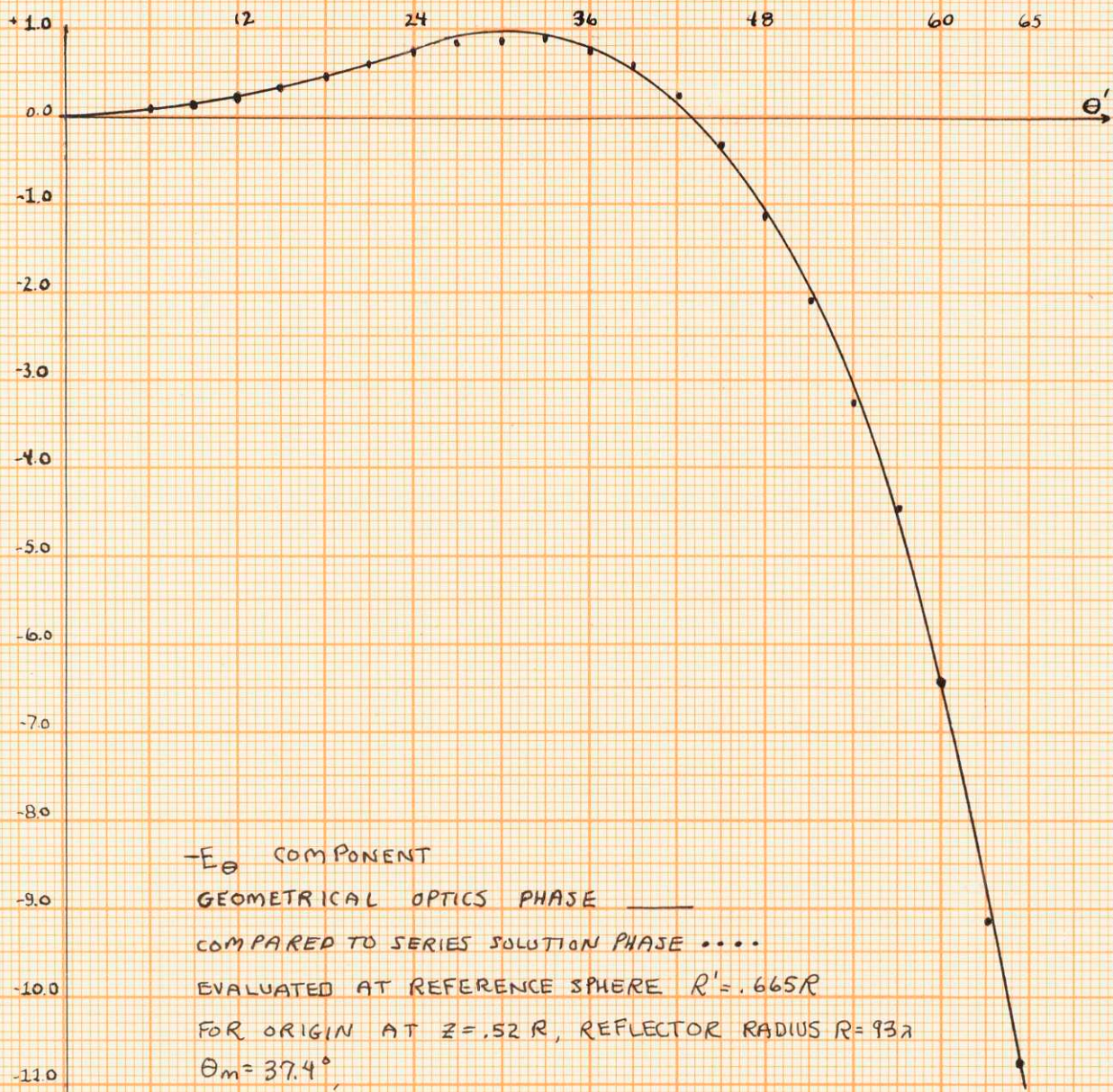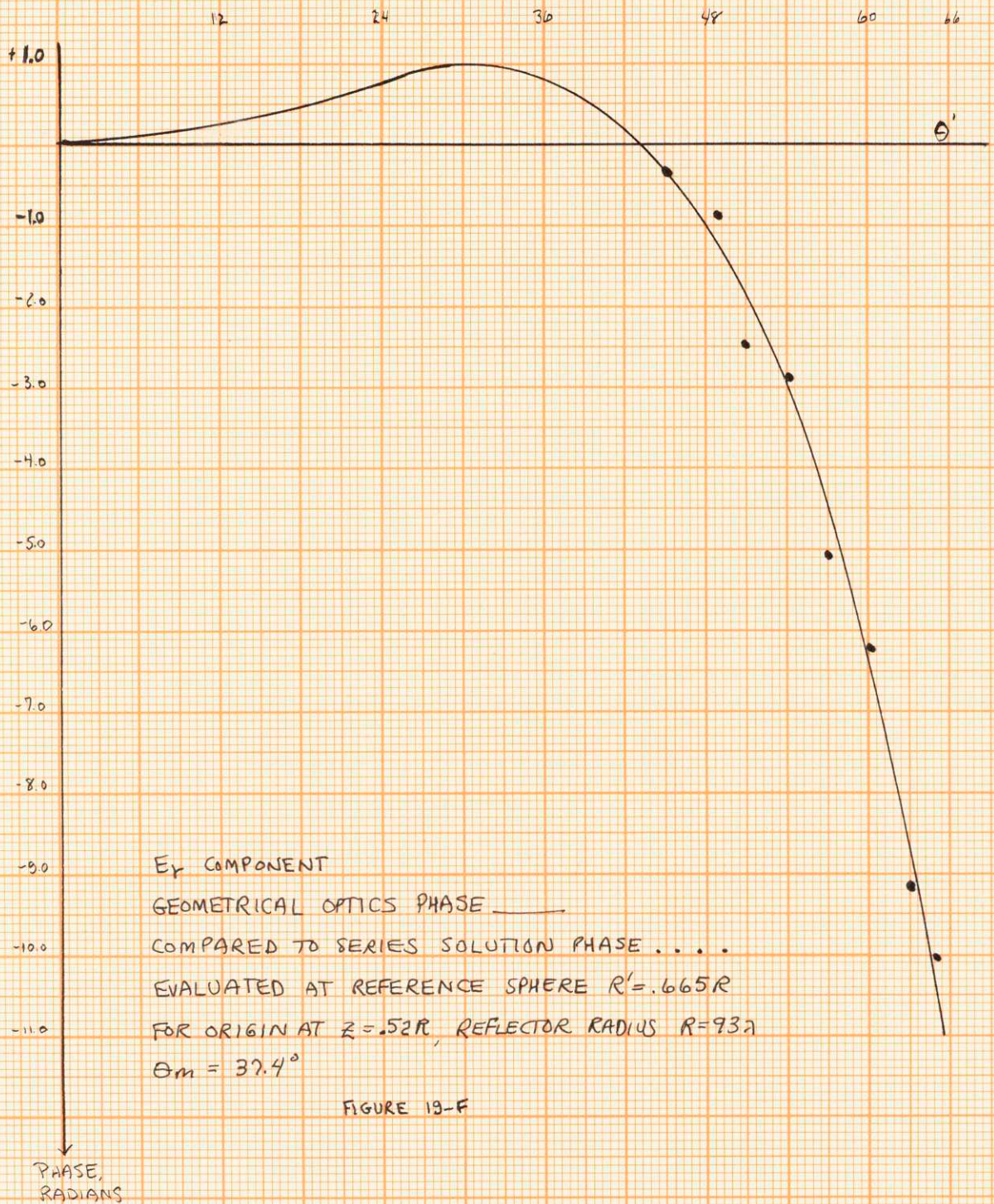RADIANS

96

CHAPTER IV

CONCLUSIONS

4.1 As noted by the graphical representation of solution offered in

figures 19, the technique explored by this thesis has yielded results

that indicate its accuracy and applicability. A geometrical optics expan-

sion from the surface of a spherical reflector to a hypothetical ref-

erence sphere can be utilizedto generate necessary coefficients required

by the series solution of spherical harmonics that constitute the

expression for the electromagnetic fields in the region of concern.

With regards to the efficiency of the technique, an investigation of

various eccentric origins from z = .5R to .6R indicated that the radii

of the ensuing reference spheres were on the order of R' = .6R for

the reflector chosen for investigation by this thesis. Thus, evaluation

of the series solution at the reference sphere for purposes of compar-

ison to the initially determined geometrical optics field involved a

reduction in the number of terms that would have been required without

the eccentric coordinate system by some 40 %. The reduction in terms is

due to the direct relationship between the radius of observation and the

number of terms required. Due to the flexible nature of the technique,

choice of eccentric origin to include regions of energy concentration

near the feed sphere result in the feed radius on the order of 8 λ

for the reflector of 93 λ considered by this study.

Previous investigation [43] constrained by a fixed origin and con-
centric spheres, as given by figure 2, found it necessary to keep the
radius of the feed sphere on the order of half the radius of the reflec-
tor. Thus we consider that this technique has provided a substantial
reduction in the number of terms involved from

$$M = kr = (\ 2\pi/\lambda \ )(\ 93\lambda \ /2)$$

to

$$M = kr = (\ 2\pi/\lambda \ ) \ 8 \ \lambda$$

indicating a savings of a factor of approximately an order of magnitude.

4.2   A next logical step in pursuance of this technique

would be to concentrate on the series solution at the

radii of various feed spheres. This study suggests that

if the fields given by figure 16 can be duplicated over

the surface of the feed sphere by some source within the

sphere the desired illumination of uniform plane wave

over the aperture of the reflector will be realized. The

calculation of the fields at the aperture by an alternative

measurement technique, or by experimental methods, if the

fields over the feed sphere can be realized by some practi-

cal feed system, would be a most worthwhile endeavor.

Further study for a series of parameter variations for

one reflector could, as well, yield a meaningful extension

of this technique. Based upon the field distribution over

the feed sphere, design and experimentation with a feed

system could provide the basis for additional study of this

topic at various academic levels of concern.

APPENDIX I

SIMPLIFICATION AND MANIPULATIVE DETAILS OF CERTAIN EXPRESSIONS

Derivation of Equation 2.12

From equation 2.11:

$$N/\rho = - S \times \nabla \times S \qquad\qquad A.1$$

Taking the dot product with N to both sides of A.1

$$1/\rho = -N \cdot S \times \nabla \times S$$

applying the vector identity

$$A \cdot (B \times C) = C \cdot (A \times B)$$

then

$$1/\rho = - (N \times S) \cdot (\nabla \times S) \qquad\qquad A.2$$

By equation 2.10

$$S = \nabla L/\eta$$

Substituting and operating:

$$\nabla \times S = \nabla \times \frac{\nabla L}{\eta} = \nabla \frac{1}{\eta} \times \nabla L + \frac{1}{\eta} \nabla \times \nabla L$$

But $\nabla \times \nabla L = 0$ so

$$\nabla \times S = \nabla \frac{1}{\eta} \times \nabla L \qquad\qquad A.3$$

Substituting A.3 into A.2:

$$1/\rho = -(N \times S) \cdot (\nabla \frac{1}{\eta} \times \nabla L) \qquad\qquad A.4$$

We substitute

$$\nabla \frac{1}{\eta} = - \frac{1}{\eta} \nabla (\ln \eta)$$

$$1/\rho = -(N \times S) \cdot (- \frac{1}{\eta} \nabla (\ln \eta) \times \nabla L) \qquad A.5$$

But by the vector identity

$$A \times B \cdot C \times D = (A \cdot C)(B \cdot D) - (A \cdot D)(B \cdot C)$$

A.6
$$1/\rho = \frac{1}{\eta}(\ (N\cdot\nabla\ln\ \eta)(S\cdot\nabla L)\ -\ (N\cdot\nabla L)(S\cdot\nabla\ln\ \eta)\ )$$

From 2.10, where $S\cdot\nabla L = \dfrac{|\nabla L|^2}{\eta} = \eta$

$$1/\rho = \frac{1}{\eta}(\ N\cdot\nabla\ln\ \eta\ -\ (N\cdot\nabla L)(S\cdot\nabla\ln\ \eta)\qquad \text{A.7}$$

The second term in A.7 is identically zero since by A.1

$$N = -\ \rho(S\ x\ \nabla\ x\ S)$$

and from 2.10

$$\nabla L = S\eta$$

then substituting the above into the second term:

$$\frac{(N\cdot\nabla L)}{\rho\eta} = -S\cdot(S\ x\ \nabla\ x\ S)$$

Again using the vector identity

$$A\cdot(B\ x\ C) = C\cdot(A\ x\ B)$$

we see

$$\nabla \times S \cdot (S \times S) = 0$$

Therefore, from A.7

$$1/\rho = N \cdot \nabla \ln \eta \qquad\qquad A.8 = 2.12$$

Derivation of equation 2.37 '

From equation 2.34

$$x = (z - z_o) \tan 2\theta$$
$$x^2 = (z^2 - 2zz_o + z_o^2) \tan^2 2\theta \qquad\qquad A.9$$

From equation 2.35

$$R'^2 = x^2 + z^2 - 2zcR + c^2 R^2 \qquad\qquad A.10$$

Substitution of A.9 into A.10

$$R'^2 = (z^2 - 2zz_o + z_o^2)\tan^2 2\theta + z^2 - 2zcR + c^2 R^2$$

A.11
$$= (\tan^2 2\theta + 1)z^2 - 2z(z_o \tan^2 2\theta + cR) + z_o^2 \tan^2 2\theta + c^2 R^2$$

Multiplying A.11 by $\cos^2 2\theta$

$$R'^2 \cos^2 2\theta = (\sin^2 2\theta + \cos^2 2\theta)z^2 - 2z(z_0 \sin^2 2\theta + cR\cos^2 2\theta)$$

$$+ z_0^2 \sin^2 2\theta + c^2 R^2 \cos^2 2\theta \qquad\qquad A.12$$

Solving A.12 for z :

$$0 = z^2 - 2z(z_0 \sin^2 2\theta + cR\cos^2 2\theta) + z_0^2 \sin^2 2\theta - \cos^2 2\theta(R'^2 - c^2 R^2) \quad A.13$$

From 2.36:

$$\frac{R}{\sin 2\theta} = \frac{z_0}{\sin\theta}$$

$$z_0 = \frac{\sin\theta}{\sin 2\theta} R \qquad\qquad A.14$$

Substituting A.14 into A.13 :

$$z^2 - 2z(\sin\theta\sin 2\theta R + cR\cos^2 2\theta) + \sin^2\theta R^2 - \cos^2 2\theta(R'^2 - c^2 R^2) = 0$$
$$A.15$$

Normalizing A.15 to the radius of reflector R:

$$z_n = \frac{z}{R} \quad , \quad R_n' = \frac{R'}{R}$$

$$z_n^2 - 2z_n(\sin\theta\sin2\theta + c^2\cos^2 2\theta) + \sin^2\theta - \cos^2 2\theta \, (R_n'^2 - c^2) = 0, \qquad A.16 = 2.37$$

Derivation of equations 2.43, 2.44

Normalizing equation 2.41, 2.42:

$$R_{1n} = \sqrt{(z_{mn} - z_{cn})^2 + (x_{mn} - x_{cn})^2} \qquad A.17$$

where

$$z_{mn} = \cos\theta$$

$$x_{mn} = \sin\theta$$

$$z_{cn} = \frac{1}{4}(3\cos\theta - \cos3\theta)$$

$$x_{cn} = \frac{1}{4}(3\sin\theta - \sin3\theta)$$

$$z_{on} = \frac{\sin\theta}{\sin2\theta}$$

Substitution and expanding A.17:

$$R^2_{1n} = \left(\frac{\cos\theta}{4} + \frac{\cos3\theta}{4} \right)^2 + \left(\frac{\sin\theta}{4} + \frac{\sin3\theta}{4} \right)^2 \qquad \text{A.18}$$

$$= \frac{1}{16} \left(2\cos\theta\cos3\theta + 2\sin\theta\sin3\theta + 2 \right)$$

$$= \frac{1}{16} \left(2 + 2\cos2\theta \right) \qquad \text{A.19}$$

but $\cos2\theta = 1 - 2\sin^2\theta$

$$R^2_{1n} = \frac{4}{16} \left(1 - \sin^2\theta \right)$$

$$R^2_{1n} = \frac{\cos^2\theta}{4}$$

then

$$R_{1n} = \frac{\cos\theta}{2} \qquad \text{A.20=2.41}$$

Similarly, by expanding 2.42:

$$R^2_{2n} = \left(\cos\theta - \frac{\sin\theta}{\sin2\theta} \right)^2 + \sin^2\theta \qquad \text{A.21}$$

$$= \cos^2\theta + \sin^2\theta + \frac{\sin\theta}{\sin^2 2\theta} - \frac{2\cos\theta\sin\theta}{\sin2\theta}$$

$$R_{2n}^2 = 1 - 1 + \frac{\sin\theta}{\sin 2\theta}$$

Then

$$R_{2n} = \frac{1}{2\cos\theta} \qquad\qquad\qquad A.22= 2.44$$

APPENDIX II

COMPUTATIONAL TECHNIQUES RELEVANT TO PROBLEM SOLUTION

As noted in section 2.5, expressions for fields were programmed in FORTRAN to yield a numerical solution to equation 2.52. A copy of the program utilized follows this discussion. Briefly, the logical progression is outlined:

1. For a given reflector of radius R and subtended angle Θ_m, equation 2.31 is used to calculate the reference sphere radius R' for a particular choice of parameter c.

2. Equation 2.40 is programmed to yield the angle θ' measured from the new origin at z=cR to points on the reference sphere corresponding to rays incident upon the reflector surface at a given angle θ. A one-to-one correspondence is established between the angles.

3. Equations 2.41 and 2.42 are programmed along with 2.33 to yield values for the field amplitude at various angles θ', measured from the new origin, on the surface of the reference sphere. The amplitude expression is then given by the inverse distance relationship of the form of equation 2.17.

4. The polarization features covered by equations 2.46-2.51 are programmed to indicate the effect of redefining the field components in the new coordinate system.

5. The phase expression is calculated for the reflector under consideration by relation 2.30 and 2.33, and the resulting phase is chosen relative to the phase at $\theta = \theta' = 0$ degrees.

6. The information generated by the previous steps is collected and output, if desired, is made available, representing a numerical solution to equation 2.52.

The graphs included in section 2.5 were prepared from results generated as described above.

It is noted, however, that the actual field on the reference sphere is only of passing interest at this point, and that expansion of this field into a cosine fourier series, as given by equation 3.14, is of paramount interest:

$$E \begin{matrix} \text{reference} \\ \text{sphere} \\ \text{tangential} \end{matrix} = \sum_{m=0}^{\infty} (c_m \cos\phi\ i_{\theta'} + d_m \sin\phi\ i_{\phi})\cos m\theta' \qquad \text{A.23}$$

The subroutine FORC was developed to generate coefficients for the fourier series from the generated field components. A numerical technique for evaluating the coefficients for such a series appropriate for a periodic set of discrete values of a function was available[44] and was used as the basis for this subroutine. As a check, the fourier series was summed, indicating accuracy to within a few percent when viewed overall and compared to the points used to generate the coefficients.

The technique follows from consideration of expansion of a periodic function $f(\theta)$ in a fourier series:

$$f(\theta) = a_0/2 + \sum_{m=1}^{\infty} a_m \cos m\theta + b_m \sin m\theta \qquad \text{A.24}$$

where from orthogonality it may easily be shown that the resultant coefficients are given by:[45]

$$a_m = \frac{1}{\pi} \int_0^{2\pi} f(\theta) \cos m\theta \, d\theta \qquad m=0, 1, \ldots. \qquad \text{A.25}$$

As the case of interest involves symmetry about $\theta = 0$, it is obvious that a cosine series will suffice to fully express the function and b_m will be identically zero for all m.

The integral expression A.25 can be related to a summation of discrete values by approximations of basic calculus, where the interval from $0 < \theta < 2\pi$ is divided into 2N intervals, providing $2N + 1$ data points. Thus we can formulate a relationship between the number of intervals and the spacing involved where

$$2N = 360^{\circ}/ \text{DEL}$$

DEL being the spacing between successive points. Thus we approximate, for a sufficiently large number of points:

$$d\theta \cong \Delta\theta = \frac{2\pi}{2N + 1}$$

$$\theta \cong n\Delta\theta = \frac{2\pi n}{2N + 1} \qquad \text{where} \quad n= 0,1,2, \ldots 2N$$

Substitution of the above approximations into A.25 results in

$$a_m \cong \frac{2}{2N + 1} \sum_{n=0}^{2N} f\left(\frac{2\pi n}{2N + 1}\right) \cos m \frac{2\pi n}{2N + 1} \qquad \text{A.26}$$

Thus we see the function must be made available in steps of angle, determined by the index n, or at the following discrete points:

$$\Theta_n = \frac{2\pi n}{2N + 1} \qquad n = 0,1,2,\ldots 2N$$

Therefore, the following steps are outlined to provide an indication of the progression followed through the subroutine:

1. Since the series requires even spacing between the data points, it was necessary to interpolate between the points generated on the reference sphere by successive steps of the angle along the reflector surface. As equation 2.40 allowed no simple inverse relationship between the two angles θ and θ', small steps of the angle on the reflector surface were taken (spacing = .2 degrees) to insure the accuracy of linear interpolation between the discrete values of angle θ' generated.

2. The resulting field expressions were arranged in component form and subsequently expanded from the exponential representation to the trigonometric form :

where $Ae^{j\psi} = A(\cos\psi + j\sin\psi) = AR + jAI$

3. The values of field components, two real and two
   imaginary, were then used to generate a complex
   fourier coefficient of the form

   $$C = CR + jCI$$

   by the technique previously described.

4. The answers of interest were these coefficients which,
   when properly inserted into an existing program for
   the series solution to field expressions 3.16 and 3.17.
   The fourier coefficients c_m and d_m are noted in equation
   3.16.

```
      DIMENSION CR(400),DR(400),DI(400),CI(400)
  109 FORMAT(1H ,'      J',3X,'     CR     ',3X,'     CI     ',
     13X,'     DR     ',3X,'     DI     ')
  108 FORMAT(1H ,I5,3X,F10.7,3X,F10.7,3X,F10.7,3X,F10.7)
  150 FORMAT(1H1,10X,'REFLECTOR RADIUS=',F10.7,3X,
     1'RADIUS OF OBSERVATION=',F10.7,3X,'REFERENCE SPHERE RADIUS=',
     2F10.7,3X,'MAX HARMONIC MAXM=',3X,I5)
C     CHOOSE INNER SPHERE COINCIDENT WITH OUTER SPHERE FOR
C     CHECK ON SERIES EXPANSION
      R1=93.
      R=.664892*93.
      C=.52
      THM=37.4
      JZ=0
      MAXM=IFIX(2.*3.141593*R)
      MO=MAXM+3
      CALL XFEED(R1,R,RAD,C,THM,MAXM,DI,DR,CR,CI,CZR,CZI,DZR,DZI)
      WRITE(6,150)R1,R,RAD,MAXM
      WRITE(6,109)
      WRITE(6,108)JZ,CZR,CZI,DZR,DZI
      WRITE(6,108) (J,CR(J),CI(J),DR(J),DI(J),J=1,MO)
      CALL EXIT
      END
      SUBROUTINE XFEED(R1,R,RAD,C,THM,MAXM,DI,DR,CR,CI,CZR,CZI,DZR,DZI)
      DIMENSION CR(1),CI(1),DR(1),DI(1)
      DIMENSION EFICMR(400),ETHCMR(400),ETHCMI(400),EFICMI(400)
      DIMENSION ETCMRA(400),EFCMRA(400),ETCMIA(400),EFCMIA(400)
      DIMENSION THP(250),ETP(250),EPP(250),PHR(250)
      DIMENSION THPI(350),PHRI(350),ETPI(350),EPPI(350)
 1000 FORMAT(1H1,28X,'THM =',F10.7,5X,'RPN =',
     1F10.7,5X,'  C =',F10.7)
 1010 FORMAT(1H ,I5,2X,F5.2,2X,F10.7,2X,F10.5,2X,F10.7,
     1'COS(PHI)',2X,F10.7,'COS(PHI)',2X,F10.7,'SIN(PHI)',
     22X,F5.2)
 1020 FORMAT(1H ,'      I',2X,' THP ',6X,'AMP',8X,'PHASE',8X,
     1'ERP',17X,'ETP',17X,'EPP',15X,'TH')
```

```fortran
  110 FORMAT(1H1,'     K',3X,' EFICMR ',3X,' EFCMRA ',
     13X,' EFICMI ',3X,' EFCMIA ',3X,' ETHCMR ',
     23X,' ETCMRA ',3X,' ETHCMI ',3X,
     3' ETCMIA ',5X,'THPI')
  111 FORMAT(1H ,I5,3X,F10.7,3X,F10.7,3X,F10.7,3X,F10.7,
     13X,F10.7,3X,F10.7,3X,F10.7,3X,F10.7,3X,F5.2)
  105 FORMAT(1H1,41X,'INTERPOLATED VALUES')
  106 FORMAT(1H '     K',3X,'THPI',5X,' PHRI ',5X,
     1' ETPI ',8X,' EPPI ')
 1030FORMAT(1H ,I5,2X,F5.2,2X,F10.5,2X,
     1F10.7,'COS(PHI)',2X,F10.7,'SIN(PHI)')
      TPI=2.*3.1415926
      CVR=TPI/360.
      DEL=.25
      N=IFIX(360./(2.*DEL))
      DTH=.2
      NTH=IFIX(THM/DTH+2.)
      THMR=THM*CVR
      RPN=SQRT(C*C+1.-2.*C*COS(THMR))
      RAD=RPN*R1
      WRITE(6,100)THM,RPN,C
      WRITE(6,102)
      TH=0.0
      DO 3 I=1,NTH
      THR=TH*CVR
      A=SIN(THR)*SIN(2.*THR)+C*(COS(2.*THR)*COS(2.*THR))
      B=A*A-SIN(THR)*SIN(THR)+(RPN*RPN-C*C)*COS(2.*THR)*COS(2.*THR)
      CTHPR=(1./RPN)*(A-C+SQRT(B))
      STHPR=SQRT(1.-CTHPR*CTHPR)
C     AMPLITUDE
C     TAPER=ILLUMINATION TAPER OF AMPLITUDE OVER APERTURE
C     AEDGE=AMPLITUDE TO WHICH TAPER DESIRED
C     TAPER=COS(AEDGE*THR)
C     AEDGE=0.0
      TAPER=1.0
      AA=SIN(THR)-RPN*STHPR
```

```
          BB=RPN*CTHPR+C-COS(THR)
          SN=SQRT(AA*AA+BB*BB)
          R1N=COS(THR)/2.
          R2N=1./(2.*COS(THR))
          AMP=SQRT(.25/(.25+SN*(R1N+R2N)+SN**2.))
          AMP=AMP*TAPER
C         PHASE FOR REFLECTOR RADIUS=R1 LAMBDA
C         PHASE CALCULATED RELATIVE TO PHR(1) AT THETA=THETA'=0
          DELP=COS(THR)-SN
          PHR(I)=R1*TPI*DELP
          PHREL=PHR(1)
          IF(I-1)6,6,7
      6   PHR(1)=0.0
          GO TO 5
      7   PHR(I)=PHR(I)-PHREL
      5   CONTINUE
C         POLARIZATION
          THPR=ARCOS(CTHPR)
          THP(I)=THPR/CVR
          THP(1)=0.0
          DIFR=2.*THR-THPR
          CDIF=COS(DIFR)
          SDIF=SIN(DIFR)
C         FIELD COMPONENTS
          ERP=AMP*SIN(DIFR)
          ETP(I)=-AMP*COS(DIFR)
          EPP(I)=AMP
          WRITE(6,101)I,THP(I),AMP,PHR(I),ERP,ETP(I),EPP(I),TH
          TH=TH+DTH
          PHR(1)=PHREL
      3   CONTINUE
C         VALUES OF FIELD ARE INTERPOLATED FOR SERIES EXPANSION
C         INTERVAL BETWEEN POINTS=DEL, IN DEGREES OF THETA'
          PHR(1)=0.0
          NTHP=IFIX(THP(NTH)/DEL+1.0)
          DO 4 K=1,NTHP
```

```
      THPI(K)=FLOAT(K-1)*DEL
      I=1
   10 IF (THPI(K)-THP(I)) 8,8,9
    9 IF (THPI(K)-THP(I+1)) 8,8,11
   11 I=I+1
      GO TO 10
    8 CONTINUE
      S=(THPI(K)-THP(I))/(THP(I+1)-THP(I))
      PHRI(K)=PHR(I)+(PHR(I+1)-PHR(I))*S
      ETPI(K)=ETP(I)+(ETP(I+1)-ETP(I))*S
      EPPI(K)=EPP(I)+(EPP(I+1)-EPP(I))*S
    4 CONTINUE
      WRITE(6,105)
      WRITE(6,106)
      WRITE(6,103)(K,THPI(K),PHRI(K),ETPI(K),EPPI(K),K=1,NTHP)
C     PHASE TERM EXPANDED INTO TRIGONOMETRIC FORM
C     WHERE A EXP JPH=A(COSPH+JSINPH)
C     ETHCMR=REAL PART OF THETA COMPONENT
C     EFICMR=REAL PART OF PHI COMPONENT
C     ETHCMI=IMAG PART OF THETA COMPONENT
C     EFICMI=IMAG PART OF PHI COMPONENT
      DO 12 I=1,NTHP
      EFICMR(I)=EPPI(I)*COS(PHRI(I))
      ETHCMR(I)=ETPI(I)*COS(PHRI(I))
      ETHCMI(I)=ETPI(I)*SIN(PHRI(I))
      EFICMI(I)=EPPI(I)*SIN(PHRI(I))
   12 CONTINUE
C     SUBROUTINE CALLED TO EVALUATE FOURIER COEFFICIENTS
C     CR(M)=REAL C(M)
C     CZR=CR(0)
C     DR(M)=REAL D(M)
C     DZR=DR(0)
C     CI(M)=IMAG C(M)
C     CZI=CI(0)
C     DI(M)=IMAG D(M)
C     DZI=DI(0)
```

```
      CALL FORC(EFICMR,N,NTHP,MAXM,DR)
      CALL FORC(EFICMI,N,NTHP,MAXM,DI)
      CALL FORC(ETHCMI,N,NTHP,MAXM,CI)
      CALL FORC(ETHCMR,N,NTHP,MAXM,CR)
      DZI=DI(1)
      CZI=CI(1)
      CZR=CR(1)
      DZR=DR(1)
      MO=MAXM+3
      DO 770 J=2,MO
      DR(J-1)=DR(J)
      CR(J-1)=CR(J)
      DI(J-1)=DI(J)
      CI(J-1)=CI(J)
  770 CONTINUE
C     CHECK FOURIER SERIES BY SUMMATION
      DO 20 K=1,NTHP
      ETCMRA(K)=CZR
      EFCMRA(K)=DZR
      ETCMIA(K)=CZI
      EFCMIA(K)=DZI
      SUM1=0.0
      SUM2=0.0
      SUM3=0.0
      SUM4=0.0
      AN=N
      CONST=2.*3.141593/(2.*AN+1.)
      DO 30 J=1,MAXM
      FFK=FLOAT(K)
      FFJ=FLOAT(J)
      COST=COS(FFJ*FFK*CONST)
      SUM1=SUM1+CR(J)*COST
      SUM2=SUM2+DR(J)*COST
      SUM3=SUM3+CI(J)*COST
      SUM4=SUM4+DI(J)*COST
   30 CONTINUE
```

```
          ETCMRA(K)=ETCMRA(K)+SUM1
          EFCMRA(K)=EFCMRA(K)+SUM2
          ETCMIA(K)=ETCMIA(K)+SUM3
          EFCMIA(K)=EFCMIA(K)+SUM4
       20 CONTINUE
          WRITE(6,110)
          WRITE(6,111) (K,EFICMR(K),EFCMRA(K),ETHCMR(K),
         1ETCMRA(K),EFICMI(K),EFCMIA(K),ETHCMI(K),
         2ETCMIA(K),THPI(K),K=1,NTHP)
          RETURN
          END
          SUBROUTINE FORC(FNT,N,NTHP,MAXM,A)
    C     EXPANSION OF A FUNCTION GENERATED BY A SET OF
    C     DISCRETE POINTS INTO A FOURIER COSINE SERIES
    C     WHERE F(X)= A(0)+SUM A(J)COSJX,  J=1,MAXM
          DIMENSION A(1),FNT(1)
      500 FORMAT(1H1,'N NOT GREATER THAN MAXM, ORDER OF HIGHEST HARMONIC-
         1DOES NOT COMPUTE')
    C     CHECK FOR PARAMETER ERRORS
          M=MAXM+3
          IER=0
       40 IF(M-N)  60,60,50
       50 IER=1
          WRITE(6,500)
          RETURN
    C     COMPUTE AND PRESET CONSTANTS
       60 AN=N
          COEF=2.0/(2.*AN+1.)
          CONST=3.141593*COEF
          S1=SIN(CONST)
          C1=COS(CONST)
          C=1.
          S=0.0
          J=1
          FNTZ=FNT(1)
       70 U2=0.0
```

```
      U1=0.0
      I=NTHP
C     FORM FOURIER COEFFICIENTS RECURSIVELY
   75 U0=FNT(I)+2.*C*U1-U2
      U2=U1
      U1=U0
      I=I-1
      IF(I-1) 80,80,75
   80 A(J)=COEF*(FNTZ+C*U1-U2)*2.
      IF(J-(M+1)) 90,100,100
   90 Q=C1*C-S1*S
      S=C1*S+S1*C
      C=Q
      J=J+1
      GO TO 70
  100 A(1)=A(1)*.5
      RETURN
      END
```

BIBLIOGRAPHY

1. J.D. Kraus, <u>Radio Astronomy</u>, McGraw-Hill, New York, 1966, pp. 209-210.

2. M. Kline and I.W. Kay, <u>Electromagnetic Theory and Geometrical Optics</u>, John Wiley and Sons, New York, 1965, pp. 3-5.

3. J. Ashmead and A.B. Pippard, "The use of spherical reflectors as microwave scanning aerials," Journal of the IEE (London), vol. 93, part IIIA, pp. 627-632, 1946.

4. Tingye Li, "A study of spherical reflectors as wide angle scanning antennas," IRE Transactions on Antennas and Propagation, vol. AP-7, no. 3, pp. 331-336, May 1960.

5. F.S. Holt and E.L. Bouche, "A gregorian corrector for spherical reflectors," IEEE Transactions on Antennas and Propagation, vol. AP-12, no. 1, pp. 44-47, January 1964.

6. R.C. Spencer, C.J. Sletten, and J.E. Walsh, "Correction of spherical aberration by a phased line source," Proceedings of the National Electronics Conference, vol. V, pp. 320-333, 1949.

7. A.C. Schell, "The diffraction theory of large aperture spherical reflector antennas," IEEE Transactions on Antennas and Propagation, vol. AP-11, no. 4, p. 428, July 1963.

8. L. LaLonde and D.E. Harris, "A high performance line source feed for the AIO spherical reflector," IEEE Transactions on Antennas and Propagation, vol. AP-17, no. 7, p. 41, January 1970.

9. A.W. Love, "Spherical reflecting antenna with corrected line sources,"
   IRE Transactions on Antennas and Propagation, vol. AP-10, no. 5,
   p. 529-537, September 1962.

10. Reference 7, pp.428-432.

11. M.H. Cohen and G.E. Perona, "A correcting feed at 611 MHz for the
    AIO reflector," IEEE Transactions on Antennas and Propagation (Com-
    munications), vol. AP-15, pp. 482-483, May 1967.

12. Reference 8, p. 41

13. G.C. McCormick, "A line source feed for a spherical reflector,"
    IEEE Transactions on Antennas and Propagation, vol. AP-15, no. 5,
    pp. 639-645, September 1967.

14. A.W. Love and J.J. Gustinic, "Line source feeds for a spherical
    reflector," IEEE Transactions on Antennas and Propagation (Communica-
    tions), vol. AP-16, pp. 132-143, January 1968.

15. Reference 8, pp. 41-48.

16. L.J. Ricardi,"A method of synthesizing the fields of a feed for a
    spherical reflector," PhD. dissertation, Northeastern University,
    Boston, Massachusetts, May 1969.

17. Reference 14, p. 132

18. C.J. Sletten and W.G. Mavroides, "A Method of Sidelobe Reduction,"
    Naval Research Laboratory Report NRL-403, Washington, D.C., April
    1952.

19. M.L. Burrows and L.J. Ricardi, "Aperture feed for a spherical reflector," IEEE Transactions on Antennas and Propagation, vol. AP-15, no. 2, pp. 227-230, March 1967.

20. R.C. Spencer and G. Hyde, "Studies of the focal region of a spherical reflector," IEEE Transactions on Antennas and Propagation, vol. AP-16, numbers 3, 4, and 6, pages 317-324, 399-404, 646-656, May, July and November 1968.

21. D.F. Bowman, "Transverse Antenna Feeds," Air Force Cambridge Research Labs., Final Report, contract AF19(628)2758, January 1966.

22. H.C. Minnett and B. MacA. Thomas, "Fields in the image space of symmetrical focussing reflectors," Proceedings of the IEE (London), vol. 115, pp. 1419-1430, October 1968.

23. B. MacA. Thomas, H.C. Minnett and V.T. Bao, "Fields in the focal region of a spherical reflector," IEEE Transactions on Antennas and Propagation (Communications), vol. AP-17, no. 1, pp. 229-232, March 1969.

24. Reference 16.

25. Reference 16, pp. 90-100.

26. S. Silver, Microwave Antenna Theory and Design, McGraw-Hill, New York, 1949, pp. 80-84.

27. Reference 26, pp. 107-110.

28. D. E. Christie, Intermediate College Mechanics, McGraw-Hill, New York, 1952, pp. 310-312.

29. Reference 28, pp. 115-116.

30. Reference 26, pp. 113-114.

31. Reference 26, pp. 116-118.

32. M. Born and E. Wolf, Principles of Optics, 1st Edition, Pergamon Press New York, 1959, pp. 108-129.

33. Reference 3.

34. R.F. Harrington, Time-Harmonic Fields, McGraw-Hill, New York, 1961, pp. 263-266.

35. Reference 34, pp. 267-268.

36. Reference 34, p. 268.

37. S. A. Schelkunoff, Electromagnetic Waves, D. Van Nostrand Co., Princeton, N.J., 1943, pp. 51-52.

38. P.M. Morse and H. Feshback, Methods of Theoretical Physics, Volume II, McGraw-Hill, New York, 1953, page 1766.

39. Reference 34, pp. 273-276.

40. Reference 34, pp. 468-470.

41. Reference 16, pp. 23-33, 85-88, 135-138.

42. L.J. Chu, "Physical limitations of omnidirectional antennas," Journal of Applied Physics, vol.19, 1948, pp. 1163-1175.

43. Reference 16, page 40.

44. A. Ralston, An Introductory Course in Numerical Analysis, McGraw-Hill Company, New York, 1965, p.194.

45. C. R. Wylie, Advanced Engineering Mathematics, McGraw-Hill, New York, 1960, Chapter 7.